

Benders decomposition for the large-scale probabilistic set covering problem

Jie Liang^{a,b,c}, Cheng-Yang Yu^a, Wei Lv^a, Wei-Kun Chen^{a,b}, and Yu-Hong Dai^{c,d}

^a*School of Mathematics and Statistics, Beijing Institute of Technology, Beijing 100081, China, {liangjie,yuchengyang,lwei,chenweikun}@bit.edu.cn*

^b*State Key Laboratory of Cryptology, P. O. Box 5159, Beijing, 100878, China*

^c*Sichuan Aerospace Chuannan Initiating Explosive Technology Limited, Luzhou 646000, China*

^d*Academy of Mathematics and Systems Science, Chinese Academy of Sciences, Beijing 100190, China*

^e*School of Mathematical Sciences, University of Chinese Academy of Sciences, Beijing 100049, China, dyh@lsec.cc.ac.cn*

Abstract

In this paper, we consider a probabilistic set covering problem (PSCP) in which each 0-1 row of the constraint matrix is random with a finite discrete distribution, and the objective is to minimize the total cost of the selected columns such that each row is covered with a pre-specified probability. We develop an effective decomposition algorithm for the PSCP based on the Benders reformulation of a standard mixed integer programming (MIP) formulation. The proposed Benders decomposition (BD) algorithm enjoys two key advantages: (i) the number of variables in the underlying Benders reformulation is equal to the number of columns but independent of the number of scenarios of the random data; and (ii) the Benders feasibility cuts can be separated by an efficient polynomial-time algorithm, which makes it particularly suitable for solving large-scale PSCPs. We enhance the BD algorithm by using initial cuts to strengthen the relaxed master problem, implementing an effective heuristic procedure to find high-quality feasible solutions, and adding mixed integer rounding enhanced Benders feasibility cuts to tighten the problem formulation. Numerical results demonstrate the efficiency of the proposed BD algorithm over a state-of-the-art MIP solver. Moreover, the proposed BD algorithm can efficiently identify optimal solutions for instances with up to 500 rows, 5000 columns, and 2000 scenarios of the random rows.

Keywords: Large-scale optimization · Benders decomposition · probabilistic set covering problem · mixed integer programming Location

1 Introduction

Given a 0-1 $m \times n$ matrix A and an n -dimensional vector c representing the cost of the columns, the set covering problem (SCP) is to seek a subset of columns such that the sum of the costs of the selected columns is minimized while covering all rows of matrix A . The mathematical formulation for the SCP (Toregas et al., 1971) can be written as

$$\min \{c^\top x : A_i x \geq 1, \forall i \in [m], x \in \{0, 1\}^n\}, \quad (\text{SCP})$$

where A_i is the i -th row of matrix A , variable x_j takes value 1 if column j is selected and 0 otherwise, and $[m] := \{1, \dots, m\}$ (throughout the paper, for a nonnegative integer k , we denote $[k] = \{1, \dots, k\}$ where $[k] = \emptyset$ if $k = 0$). The SCP is one of the fundamental combinatorial optimization problems, and serves as a building block in various applications, such as facility location, manufacturing, vehicle routing, railway and airline crew scheduling, among many others. We refer to the recent surveys Farahani et al. (2012); García & Marín (2019) and the references therein for a detailed discussion of the SCP and its various exact and heuristic algorithms.

In this paper, we consider the probabilistic set covering problem (PSCP) in which each A_i is a Bernoulli random vector, and the objective is to find a minimum-cost collection of columns that covers each row i with a probability at least $1 - \epsilon_i$:

$$\min \{c^\top x : \mathbb{P}\{A_i x \geq \mathbf{1}\} \geq 1 - \epsilon_i, \forall i \in [m], x \in \{0, 1\}^n\}. \quad (\text{PSCP})$$

Here, $\epsilon_i \in (0, 1)$, $i \in [m]$, are prespecified reliability labels. As opposed to the SCP, the PSCP can effectively capture the uncertainty of the “coverage” arising in many applications. For example, in the surveillance problem, there is a nontrivial probability that sensor j will be able to detect target i (Ahmed & Papageorgiou, 2013); in the location of emergency services, the event of a facility located at location j to provide service to a customer i is uncertain due to the variability of the traveling time (Beraldi & Bruni, 2010); in the airline crew-scheduling problem, the event of a crew covering a flight is uncertain due to the possible crew no-shows (Fischetti & Monaci, 2012).

Observe that (PSCP) is an individual probabilistic programming formulation (Charnes et al., 1958) where each individual constraint is required to be satisfied with a prespecified probability. Another approach to capture the uncertainty of the “coverage” in the SCP is to use the joint probabilistic programming framework; see, e.g., Ruszczyński (2002); Luedtke (2014); Lejeune & Margot (2016); Hu et al. (2022); Küçükyavuz & Jiang (2022); Jiang & Xie (2022) among many of them. In this framework, the m probabilistic constraints in (PSCP) are replaced by a *joint* probabilistic constraint $\mathbb{P}(Ax \geq \mathbf{1}) \geq 1 - \epsilon$ ($\epsilon \in (0, 1)$), where $\mathbf{1}$ is the m -dimensional all-ones vector. Compared with the joint probabilistic programming framework, the individual probabilistic programming framework allows for the inhomogeneous reliability levels ϵ_i for different rows (Klein Haneveld et al., 2020, Chapter 5) and thus it is more flexible in many applications. For example, in the aforementioned applications, some targets, customers, or flights are usually much important than others, and thus it is reasonable to provide different reliability levels ϵ_i for the detection or coverage of them. Due to this advantage, (PSCP), the individual probabilistic programming formulation, has received many attentions in the literature. For instance, Hwang (2004) considered the case where the random coefficients a_{ij} of matrix A are independent. Fischetti & Monaci (2012) investigated the case where the random columns of matrix A are independent. Ahmed & Papageorgiou (2013) studied the case where the random coefficients in each row of matrix A are conditionally independent, meaning that the coefficients a_{ij} for $j \in [n]$ are independent when conditioned on some exogenous factors but may be correlated without such conditioning.

Unlike the existing works, we do not assume any independent or special correlated distributions of A_i in (PSCP). Instead, we consider general finite discrete distributions of A_i , that is, each A_i has a finite number of scenarios. The assumption of finite discrete distributions is not restrictive as by taking an independent Monte Carlo sampling from general distributions of A_i , we can obtain a problem that satisfies this assumption and can be treated as a sample average approximation (SAA) of (PSCP) with general distributions (Kleywegt et al., 2002). We refer to Nemirovski & Shapiro (2006); Luedtke & Ahmed (2008) for the theoretical and empirical evidence demonstrating that solving this sampling version can approximately solve the original problem with general distributions of A_i .

(PSCP) with finite numbers of scenarios of A_i can be transformed into a deterministic mixed integer programming (MIP) formulation, known as the big- M formulation (Küçükyavuz & Jiang, 2022), which can be solved to global optimality using general-purpose MIP solvers. However, due to the intrinsic NP-hardness, and particularly the huge number of binary variables and constraints (one for every scenario of A_i) and weak linear programming (LP) relaxation of the big- M formulation, the above approach cannot solve problem (2) exactly or return a high-quality solution within a reasonable timelimit, especially when the number of scenarios is large.

1.1 Contributions and Outlines

The main motivation of this work is to fill this research gap, i.e., to develop an efficient Benders decomposition (BD) algorithm for solving large-scale PSCPs. Two key features of the proposed BD algorithm, are (i) the number of variables in the Benders reformulation of the big- M formulation is equal to the number of columns n but independent of the number of scenarios of the random rows; and (ii) the Benders feasibility cuts can be separated by an efficient polynomial-time algorithm, which renders it particularly suitable to solve large-scale PSCPs, compared with the direct use of the state-of-the-art general-purpose MIP solvers.

We summarize two technical contributions of the paper as follows.

- We show that how the PSCP relates to the partial set covering problem investigated in Daskin & Owen (1999); Cordeau et al. (2019). In particular, the MIP formulation of the partial set covering problem can be seen as a special case of the big- M MIP formulation of the PSCP. Based on this observation, we generalize the single-cut BD algorithm proposed by Cordeau et al. (2019) for solving the partial set covering problem and present an efficient multi-cut BD algorithm for solving the PSCP.
- We propose three enhancement techniques to improve the performance of the proposed BD algorithm. These techniques include using initial cuts to strengthen the relaxed master problem, implementing an effective heuristic procedure to find a high-quality feasible solution, and developing mixed integer rounding (MIR)-enhanced Benders feasibility cuts to tighten the formulation of the PSCP.

Numerical results demonstrate that the proposed enhancement techniques can effectively improve the formulation of the PSCP or enable to find a high-quality solution, thereby significantly improving the overall performance of the BD algorithm; the proposed BD algorithm significantly outperforms a state-of-the-art MIP solver’s branch-and-cut and automatic BD algorithms. In particular, the proposed BD algorithm enables to quickly identify optimal solutions for PSCPs with up to 500 rows, 5000 columns, and 2000 scenarios of the random rows.

The rest of the article is organized as follows. In Section 1.2, we review the relevant literature on the PSCP. In Section 2, we introduce the MIP formulation for the PSCP, discuss the relation to the partial set covering problem, and demonstrate the difficulty of solving it. In Section 3, we present the BD algorithm for the PSCP. In Section 4, we develop three enhancement techniques for the BD algorithm. In Section 5, we perform numerical experiments to demonstrate the efficiency of the proposed enhancement techniques and the BD algorithm for the PSCP. Finally, we summarize the conclusions in Section 6.

1.2 Literature Review

(PSCP) belongs to the class of chance-constrained programs (CCPs), which have been extensively studied in the literature; see Ahmed & Shapiro (2008); Birge & Louveaux (2011); Küçükyavuz & Jiang (2022) for detailed reviews of CCPs. From a computational perspective, CCPs are challenging to solve due to the following two difficulties. First, given a point x , checking the feasibility of x could be computationally demanding. Second, the feasible region defined by the probabilistic constraints is generally nonconvex. To address the above two challenges, the SAA approach can be used where an approximation problem based on an independent Monte Carlo sample of the random data is solved to obtain a high-quality solution of the original problem. The main advantage of the SAA approach is its generality as it only requires to be able to sample from this distribution of the random data but does not require knowledge of the distribution. In this paper, we also use the SAA approach to tackle PSCPs with a general distribution of the random data $\{A_i\}$. It should be mentioned that in addition to the SAA approach, various conservative approximation approaches have been proposed in the literature; see, e.g., Nemirovski & Shapiro (2007); Ben-Tal et al. (2009); Xie & Ahmed (2020); Jiang & Xie (2022). These approaches attempt to approximate the original problem as a convex optimization problem, which is computationally tractable and can usually produce high-quality feasible solutions. Unfortunately, for CCPs with discrete variables (such as the considered PSCP), the above approximations may still be difficult to solve as the resultant feasible regions are still nonconvex.

For the probabilistic version of SCPs, let us consider a more general case of the covering constraints $A_i x \geq \xi_i$, where $A_i \in \{0, 1\}^n$ and $\xi_i \in \{0, 1\}$, $i \in [m]$, may be random. Based on the uncertainty in the covering constraints $A_i x \geq \xi_i$, $i \in [m]$ (or equivalently, $Ax \geq \xi$), the PSCP variants can generally be classified into two categories: (i) uncertainty arises in the right-hand side $\xi \in \{0, 1\}^m$; and (ii) uncertainty arises in the constraint matrix $A \in \{0, 1\}^{m \times n}$. Beraldi & Ruszczyński (2002) first studied the joint probabilistic set covering problem, in which there is a single joint chance constraint and the uncertainty arises in the right-hand side ξ :

$$\min \{c^\top x : \mathbb{P}\{Ax \geq \xi\} \geq 1 - \epsilon, x \in \{0, 1\}^n\}. \quad (1)$$

The authors developed a specialized branch-and-bound algorithm, which involves enumerating the so-called $(1 - \epsilon)$ -efficient point and solving a deterministic SCP for each $(1 - \epsilon)$ -efficient point. Subsequently, Saxena et al. (2010) developed an equivalent MIP formulation for problem (1) and derived polarity cuts to improve the computational efficiency. Luedtke & Ahmed (2008) studied problem (1) with a finite discrete distribution of the random vector ξ and proposed a preprocessing technique to improve the performance of employing MIP solvers in solving the equivalent big- M formulation. Chen et al. (2024) further proposed an efficient BD algorithm for solving large-scale problems.

For the problem with uncertainty on the constraint matrix A , as considered in this paper, Hwang (2004) and Fischetti & Monaci (2012) investigated the cases in which the random coefficients a_{ij} of matrix A and the random columns of matrix A are independent, respectively. In both cases, (PSCP) can be equivalently formulated as a compact MIP problem and thus can be solved to optimality by general-purpose MIP solvers. Ahmed & Papageorgiou (2013) established a compact mixed integer nonlinear programming formulation for (PSCP) where the random coefficients in each row of matrix A are conditionally independent. Beraldi & Bruni (2010) proposed a specialized branch-and-bound algorithm to solve the joint PSCP in which there is a single joint chance constraint and the random matrix A has a finite discrete distribution of A , that is, $\min \{c^\top x : \mathbb{P}\{Ax \geq 1\} \geq 1 - \epsilon, x \in \{0, 1\}^n\}$. Song & Luedtke (2013) developed several branch-

and-cut approaches for solving the joint PSCP reformulated from the reliable network design problem. Wu & Kucukyavuz (2019) investigated the joint probabilistic partial set covering problem and developed a delay constraint generation algorithm. Ahmed & Papageorgiou (2013); Lutter et al. (2017); Shen & Jiang (2023); Jiang & Xie (2024) investigated various robust PSCPs. We refer to Azizi et al. (2022) for more PSCP variants and their applications in location problems.

Recently, the BD algorithm has been applied to solve various large-scale SCP variants, including the partial set covering and maximal covering location problems (Cordeau et al., 2019), the probabilistic partial set covering problem (Wu & Kucukyavuz, 2019), the maximum availability service facility location problem (Muffak & Arslan, 2023), the capacitated and uncapacitated facility location problems (Fischetti et al., 2016, 2017; Wenginger & Wolsey, 2023), and the location problems with interconnected facilities (Kuzbakov & Ljubić, 2024). We refer to Rahmaniani et al. (2017) for a detailed survey of the BD algorithm and its application in many optimization problems. Special attention should be paid to the partial set covering problem considered in Cordeau et al. (2019), which minimizes the cost of the selected columns while forcing a certain amount of (weighted) rows to be covered. Cordeau et al. (2019) proposed an efficient BD algorithm that is capable of solving instances with 100 columns and up to 40 million rows. In this paper, we show that the MIP formulation of this problem can be seen as a special case of the big- M formulation of (PSCP) (with $m = 1$), and extend the BD algorithm of Cordeau et al. (2019) for this special case to the general case. Moreover, to overcome the weakness of the LP relaxation that appears in the general problem (PSCP), we propose three enhancement techniques that significantly improve the performance of the BD algorithm.

2 Mixed integer programming formulation

Consider (PSCP) with finite discrete distributions of random vectors A_i , $i \in [m]$, that is, for each i , there exist vectors $A_i^\omega \in \{0, 1\}^n$ and $p_i^\omega > 0$, $\omega \in [s]^1$, such that

$$\mathbb{P}\{A_i = A_i^\omega\} = p_i^\omega, \quad \forall \omega \in [s], \quad \text{and} \quad \sum_{\omega \in [s]} p_i^\omega = 1.$$

We introduce binary variables z_i^ω for $i \in [m]$ and $\omega \in [s]$, where $z_i^\omega = 1$ guarantees that in scenario ω , $A_i^\omega x \geq 1$ holds. Then, (PSCP) can be written as the following MIP formulation:

$$\begin{aligned} \min \quad & c^\top x \\ \text{s.t.} \quad & A_i^\omega x \geq z_i^\omega, & \forall i \in [m], \omega \in [s], \end{aligned} \tag{2a}$$

$$\sum_{\omega \in [s]} p_i^\omega z_i^\omega \geq 1 - \epsilon_i, \quad \forall i \in [m], \tag{2b}$$

$$x_j \in \{0, 1\}, \quad \forall j \in [n], \tag{2c}$$

$$z_i^\omega \in \{0, 1\}, \quad \forall i \in [m], \omega \in [s]. \tag{2d}$$

If $z_i^\omega = 1$, (2a) enforces $A_i^\omega x \geq 1$; otherwise, it reduces to the trivial inequality $A_i^\omega x \geq 0$. Constraints (2a) are referred to as big- M constraints where the big- M coefficients are given by 1; see Küçükyavuz & Jiang (2022). Notice that constraints (2a), (2b), and (2d) ensure that the probability $\mathbb{P}\{A_i x \geq 1\}$ is at least $1 - \epsilon_i$.

¹For simplicity of exposition, here we assume that the numbers of scenarios of A_i are identical for all $i \in [m]$. The extension to the case that the numbers of scenarios of A_i are different for different i is straightforward.

Remark 1. When $m = 1$, there exists only a single constraint in (2b). In this case, problem (2) is equivalent to the partial set covering problem (Daskin & Owen, 1999; Cordeau et al., 2019) where each $j \in [n]$ and $\omega \in [s]$ corresponds to a facility and a customer, respectively, and constraint (2b) reduces to the so-called coverage constraint.

Problem (2) is an MIP problem which can be solved to optimality using the state-of-the-art MIP solvers. However, the following two difficulties make it hard to solve large-scale PSCPs efficiently using the above approach. First, as opposed to (SCP) which involves only m constraints and n variables, problem (2) involves $ms + m$ constraints and $ms + n$ variables, resulting in a problem size that is one order of magnitude larger. The large problem size leads to a large LP relaxation and a large search space, thereby making it hard for the MIP solvers to solve PSCPs efficiently, especially for the case with a large number of scenarios s . To overcome this weakness, we present the following result stating that the integrality constraints on binary variables z_i^ω in problem (2) can be relaxed; see Cordeau et al. (2019) for a similar result for the partial set covering problem.

Property 2. The optimal value of problem (2) does not change if the integrality constraints (2d) are relaxed into

$$0 \leq z_i^\omega \leq 1, \forall i \in [m], \omega \in [s]. \quad (3)$$

Proof. Let (\bar{x}, \bar{z}) be an optimal solution of problem (2) with (2d) replaced by (3) and $\mathcal{F} = \{(i, \omega) \in [m] \times [s] : 0 < \bar{z}_i^\omega < 1\}$. If $\mathcal{F} = \emptyset$, the statement follows. Otherwise, as \bar{x} , $A_i^\omega \in \{0, 1\}^n$, $A_i^\omega \bar{x}$, $(i, \omega) \in \mathcal{F}$, must be an integer value larger than or equal to 1. This implies that setting $\bar{z}_i^\omega = 1$ for all $(i, \omega) \in \mathcal{F}$ will yield another feasible solution to problem (2) with the same objective value. Therefore, the statement follows as well. \square

Based on the above property, we can bypass the first difficulty by generalizing the single-cut BD approach for the partial set covering problem (i.e., problem (2) with $m = 1$) of Cordeau et al. (2019) and propose a scalable multi-cut BD algorithm to solve problem (2) (with arbitrary m) where variables z_i^ω are projected out from the problem and replaced by the Benders feasibility cuts; see Section 3 further ahead.

The second difficulty is that the LP relaxation of problem (2) could be very weak in terms of providing a poor LP bound, as will be shown in our experiments. This is in sharp contrast to the special case $m = 1$ in which Cordeau et al. (2019) observed that the difference between the optimal value of problem (2) with $m = 1$ and that of its LP relaxation is usually very small. The weakness of the LP relaxation for the general case makes it challenging for the general-purpose MIP solvers or the coming BD approach to solve problem (2) exactly or to obtain high-quality solutions. In Section 4, we will develop three enhancement techniques to overcome this weakness.

3 Benders decomposition

In this section, we first introduce an equivalent Benders reformulation for problem (2) and then present the implementation details for solving the Benders reformulation including an efficient implementation for the separation of the Benders feasibility cuts.

3.1 Benders reformulation

Observe that for a fixed $x \in \{0, 1\}^n$, problem (2) can be decomposed into m subproblems, each of which determines whether x satisfies the probabilistic constraint $\mathbb{P}\{A_i x \geq 1\} \geq 1 - \epsilon_i$. This

observation, combined with Property 2, enables to develop a multi-cut Benders reformulation of problem (2) (also called Benders master problem):

$$\min_x \{c^\top x : B_i^r(x) \geq 0, \forall r \in \mathcal{R}(\mathcal{P}_i), i \in [m], x \in \{0, 1\}^n\}, \quad (4)$$

where for each $i \in [m]$, $\mathcal{R}(\mathcal{P}_i)$ is the set of extreme rays of polyhedron \mathcal{P}_i defined by the dual of the Benders subproblem i and $B_i^r(x) \geq 0$ refers to the corresponding Benders feasibility cuts. Note that, no Benders optimality cut is needed, as variables z_i^ω do not appear in the objective function of problem (2). Given a vector $\bar{x} \in [0, 1]^n$, the Benders subproblem i and its dual can be written as

$$\min_{z_i} \{0 : (2b), z_i^\omega \leq A_i^\omega \bar{x}, 0 \leq z_i^\omega \leq 1, \forall \omega \in [s]\}, \quad (5)$$

and

$$\max_{\pi_i, \sigma_i, \gamma_i} \left\{ (1 - \epsilon_i)\gamma_i - \sum_{\omega \in [s]} (\pi_i^\omega A_i^\omega \bar{x} + \sigma_i^\omega) : (\pi_i, \sigma_i, \gamma_i) \in \mathcal{P}_i \right\}, \quad (6)$$

where π_i^ω and σ_i^ω , $\omega \in [s]$, are the dual variables associated with constraints $z_i^\omega \leq A_i^\omega \bar{x}$ and $z_i^\omega \leq 1$, respectively, γ_i is the dual variable associated with constraint (2b), and

$$\mathcal{P}_i = \{(\pi_i, \sigma_i, \gamma_i) \in \mathbb{R}_+^s \times \mathbb{R}_+^s \times \mathbb{R}_+ : \pi_i^\omega + \sigma_i^\omega \geq p_i^\omega \gamma_i, \forall \omega \in [s]\}. \quad (7)$$

By the LP duality theory, if the dual subproblem (6) is unbounded, i.e., \mathcal{P}_i has an extreme ray $(\hat{\pi}_i, \hat{\sigma}_i, \hat{\gamma}_i)$ such that $(1 - \epsilon_i)\hat{\gamma}_i - \sum_{\omega \in [s]} (\hat{\pi}_i^\omega A_i^\omega \bar{x} + \hat{\sigma}_i^\omega) > 0$, then problem (5) is infeasible. Thus the Benders feasibility cut of subproblem i violated by the infeasible point $\bar{x} \in [0, 1]^n$ reads

$$\sum_{\omega \in [s]} (\hat{\pi}_i^\omega A_i^\omega x + \hat{\sigma}_i^\omega) \geq (1 - \epsilon_i)\hat{\gamma}_i. \quad (8)$$

To solve the LP problem (6) and obtain the Benders feasibility cut (8), we follow Cordeau et al. (2019) to use an exact combinatorial approach. In particular, let $(\pi_i, \sigma_i, \gamma_i)$ be an optimal solution of problem (6). If $\gamma_i = 0$, then we can set $\pi_i^\omega = \sigma_i^\omega = 0$ for all $\omega \in [s]$ (as their objective coefficients are nonpositive), and thus the optimal value of problem (6) is zero in this case. As a result, to determine whether problem (6) is unbounded, it is sufficient to enforce $\gamma_i > 0$ in problem (6). By normalizing $\gamma_i = 1$ in problem (6), we obtain

$$\max_{\pi_i, \sigma_i} \left\{ (1 - \epsilon_i) - \sum_{\omega \in [s]} (\pi_i^\omega A_i^\omega \bar{x} + \sigma_i^\omega) : \pi_i^\omega + \sigma_i^\omega \geq p_i^\omega, \pi_i^\omega \geq 0, \sigma_i^\omega \geq 0, \forall \omega \in [s] \right\}. \quad (9)$$

Observe that $(\pi_i, \sigma_i) \in \mathbb{R}_+^s \times \mathbb{R}_+^s$ is a feasible solution of problem (9) (with an objective value of f) if and only if $(t\pi_i, t\sigma_i, t) \in \mathbb{R}_+^s \times \mathbb{R}_+^s \times \mathbb{R}_+$ with $t > 0$ is a feasible solution of problem (6) (with an objective value of tf). Thus, problem (6) is unbounded if and only if the optimal value of problem (9) is larger than zero. It is easy to see that problem (9) is bounded and one of the optimal solutions is given by

$$(\bar{\pi}_i, \bar{\sigma}_i) = \begin{cases} (p_i^\omega, 0), & \text{if } A_i^\omega \bar{x} \leq 1; \\ (0, p_i^\omega), & \text{otherwise,} \end{cases} \quad \forall \omega \in [s]. \quad (10)$$

Thus, the Benders feasibility cut (8) reduces to

$$\sum_{\omega \in [s], A_i^\omega \bar{x} \leq 1} p_i^\omega A_i^\omega x + \sum_{\omega \in [s], A_i^\omega \bar{x} > 1} p_i^\omega \geq 1 - \epsilon_i. \quad (11)$$

Note that (11) can also be derived by combining $A_i^\omega x \leq 1$ for $\omega \in [s]$ with $A_i^\omega \bar{x} \leq 1$, $z_i^\omega \leq 1$ for $\omega \in [s]$ with $A_i^\omega \bar{x} > 1$, and (2b). Also note that if $A_i^\omega \bar{x} = 1$, we can alternatively set $(\bar{\pi}_i^\omega, \bar{\sigma}_i^\omega) = (0, p_i^\omega)$, possibly resulting in a different Benders feasibility cut with the same violation at \bar{x} . However, in our preliminary experiments, we observed that the current strategy in (10) generally enables the coming BD algorithm to return a better LP bound at the root node and thus makes a better overall performance. A similar phenomenon was also observed by Cordeau et al. (2019) in the context of solving the partial set covering problem. Due to this, we decide to set $(\bar{\pi}_i^\omega, \bar{\sigma}_i^\omega) = (p_i^\omega, 0)$ for $i \in [m]$ with $A_i^\omega \bar{x} = 1$.

3.2 Implementation

To implement the BD algorithm for solving problem (4), we adopt a branch-and-cut (B&C) approach, in which Benders feasibility cuts (11) are added on the fly at each node of the search tree (constructed by the B&C approach). This approach, known as *Branch-and-Benders-cut* (Rahmaniani et al., 2017), can be implemented within the cut callback framework available in modern general-purpose MIP solvers and has been widely applied to implement the BD algorithm for various problems; see Pérez-Galarce et al. (2014); Gendron et al. (2016); Fischetti et al. (2016); Cordeau et al. (2019); Güneş et al. (2021), among many of them.

We now discuss the separation for the Benders feasibility cuts (11) in the BD algorithm. Given a point $\bar{x} \in [0, 1]^n$, to determine whether there exists a violated Benders feasibility cut (11) for each $i \in [m]$, it is sufficient to compute $A_i^\omega \bar{x}$ for all $\omega \in [s]$ and test whether the condition $\sum_{\omega \in [s], A_i^\omega \bar{x} \leq 1} p_i^\omega A_i^\omega \bar{x} + \sum_{\omega \in [s], A_i^\omega \bar{x} > 1} p_i^\omega < 1 - \epsilon_i$ is satisfied or not. This provides an $\mathcal{O}\left(\sum_{i \in [m]} \sum_{\omega \in [s]} |\text{supp}(A_i^\omega)|\right)$ algorithm for the separation of Benders feasibility cuts (11) (for a vector $a \in \mathbb{R}^n$, we use $\text{supp}(a) = \{i \in [n] : a_i \neq 0\}$ to denote its support). However, our preliminary experiments showed that this direct row-oriented implementation for the computations of $A_i^\omega \bar{x}$ is too time-consuming, especially when the number of scenarios s is large or vectors A_i^ω are dense. To resolve this issue, we note that point \bar{x} is usually very sparse encountered in the BD algorithm. To this end, we use a *column-oriented* implementation to speed up the computations of $A_i^\omega \bar{x}$, $\omega \in [s]$. Specifically, we can compute $A_i^\omega \bar{x}$, $\omega \in [s]$, using

$$\begin{bmatrix} A_i^1 \bar{x} \\ \vdots \\ A_i^s \bar{x} \end{bmatrix} =: \mathbf{A}_i \bar{x} = \sum_{j \in [n]} [\mathbf{A}_i]_j \bar{x}_j = \sum_{j \in \text{supp}(\bar{x})} [\mathbf{A}_i]_j \bar{x}_j, \quad (12)$$

with the complexity of $\mathcal{O}\left(\sum_{j \in \text{supp}(\bar{x})} |\text{supp}([\mathbf{A}_i]_j)|\right)$, where $[\mathbf{A}_i]_j \in \mathbb{R}^s$ is the j -th column of matrix $\mathbf{A}_i \in \mathbb{R}^{s \times n}$. As $\sum_{j \in \text{supp}(\bar{x})} |\text{supp}([\mathbf{A}_i]_j)| \leq \sum_{j \in [n]} |\text{supp}([\mathbf{A}_i]_j)| = \sum_{\omega \in [s]} |\text{supp}(A_i^\omega)|$, using (12) for the computations of $A_i^\omega \bar{x}$, $\omega \in [s]$, is significantly more efficient than the direct row-oriented implementation, especially when \bar{x} is very sparse, i.e., $|\text{supp}(\bar{x})| \ll n$.

The above $\mathcal{O}\left(\sum_{i \in [m]} \sum_{\omega \in [s]} |\text{supp}(A_i^\omega)|\right)$ polynomial-time separation algorithm can also be used to detect whether problem (PSCP) (or problem (2)) has a feasible solution. Indeed, letting $x, y \in \{0, 1\}^n$ with $x \leq y$, if x is a feasible solution of problem (PSCP), then y must also be a feasible solution. Therefore, detecting whether problem (PSCP) has a feasible solution is equivalent to checking whether the all-ones vector $\mathbf{1}$ is a feasible solution of problem (PSCP). The latter can be done by checking whether the Benders feasibility cut (11) with $\bar{x} = \mathbf{1}$ is violated by vector $\mathbf{1}$ for

some $i \in [m]$. If there exist some $i \in [m]$ for which (11) with $\bar{x} = \mathbf{1}$ is violated by vector $\mathbf{1}$, i.e.,

$$\sum_{\omega \in [s], |\text{supp}(A_i^\omega)| \geq 1} p_i^\omega < 1 - \epsilon_i, \quad (13)$$

then problem (PSCP) (or problem (2)) is infeasible; otherwise, problem (PSCP) must have a feasible solution. Condition (13) reflects that if $\{\epsilon_i\}$ are very small and $\{A_i^\omega\}$ are very sparse, then problem (PSCP) is likely to be infeasible. However, as condition (13) can be quickly identified (with the complexity of $\mathcal{O}(\sum_{i \in [m]} \sum_{\omega \in [s]} |\text{supp}(A_i^\omega)|)$), we, without loss of generality, assume that problem (PSCP) has a feasible solution in the following.

To end of this section, we highlight two advantages of the proposed BD algorithm as follows. First, in contrast to the big- M formulation (2) where the number of variables is $n + ms$ and grows linearly with the number of scenarios, the number of variables in the Benders reformulation (4) is only n and thus independent of the number of scenarios s . Second, the Benders feasibility cuts (11) can be separated in an $\mathcal{O}(\sum_{i \in [m]} \sum_{\omega \in [s]} |\text{supp}(A_i^\omega)|)$ polynomial-time algorithm, along with the above acceleration technique. The above two advantages make the proposed BD algorithm particularly suitable for solving large-scale PSCPs, especially for those with a huge number of scenarios.

4 Improving performance of the Benders decomposition

In this section, we will propose three enhancement techniques to improve the performance of the proposed BD algorithm for solving PSCPs. These techniques include adding tight initial cuts to strengthen the relaxed master problem, implementing a customized relaxation enforced neighborhood search (RENS) procedure (Berthold, 2014) in the early stage of the BD algorithm to find a high-quality feasible solution, and adding MIR-enhanced Benders feasibility cuts to tighten the LP relaxation of formulation (4).

4.1 Initialization of relaxed master problem

In general, the BD algorithm can start with a relaxed version of the master problem (4) without any Benders feasibility cut added. However, previous studies have demonstrated that it is computationally advantageous to add some tight initial cuts to strengthen the relaxed master problem (Rahmaniani et al., 2017). In the context of the PSCP, we decide to add the Benders feasibility cuts (11) induced by point $x = \mathbf{0}$ (where $\mathbf{0}$ is the n -dimensional zero vector), i.e.,

$$\sum_{\omega \in [s]} p_i^\omega A_i^\omega x \geq 1 - \epsilon_i, \quad \forall i \in [m]. \quad (14)$$

to the relaxed master problem as constraints. It should be mentioned that adding constraints (14) not only strengthens the relaxed master problem but also enables MIP solvers to construct internal cuts (e.g., knapsack cover cuts) that further strengthen the LP relaxation of formulation (4) and thus improve the performance of the BD algorithm; see Section 5.4.

4.2 A customized relaxation enforced neighborhood search procedure

One drawback of the BD algorithm is that it never sees the complete formulation as a whole but only a part at a time, making it challenging to find high-quality feasible solutions in the early stage

of the algorithm; see, e.g., Botton et al. (2013); Rahmaniani et al. (2017). However, in practice, it is crucial to identify a high-quality feasible solution within a reasonable amount of time. Moreover, a high-quality feasible solution can serve as a useful upper bound that helps the BD algorithm to prune the uninteresting nodes of the search tree (i.e., those that do not contain a feasible solution better than the incumbent). In the following, we develop a customized RENS procedure, proposed in Berthold (2014) for generic MIPs, to construct a high-quality solution for problem (4).

Let x^{LP} be a feasible solution of the LP relaxation of problem (4) (which can be accessed once the BD algorithm finishes exploring the root node). The RENS procedure attempts to find the *optimal rounding* of point x^{LP} by solving a subproblem of problem (4) (Berthold, 2014). This subproblem is defined by fixing variables $x_j = 0$ for all $j \in \mathcal{N}^0$ and $x_j = 1$ for all $j \in \mathcal{N}^1$ in problem (4):

$$\min_x \{c^\top x : B_i^r(x) \geq 0, \forall r \in \mathcal{R}(\mathcal{P}_i), i \in [m], x_j = 0, \forall j \in \mathcal{N}^0, x_j = 1, \forall j \in \mathcal{N}^1, x \in \{0, 1\}^n\}, \quad (15)$$

where

$$\mathcal{N}^0 = \{j \in [n] : x_j^{\text{LP}} = 0\} \text{ and } \mathcal{N}^1 = \{j \in [n] : x_j^{\text{LP}} = 1\}, \quad (16)$$

and $B_i^r(x) \geq 0, \forall r \in \mathcal{R}(\mathcal{P}_i), i \in [m]$, are all Benders feasibility cuts of the form (11). As this subproblem is a restriction of problem (4), it can still be solved by the BD algorithm. Moreover, solving subproblem (15) always returns a feasible solution.

Proposition 3. *Let x^{LP} be a feasible solution of the LP relaxation of problem (4), and \mathcal{N}^0 and \mathcal{N}^1 be defined as in (16). Then subproblem (15) has a feasible solution.*

Proof. As $p_i^\omega > 0$ and $A_i^\omega \in \{0, 1\}^n$, each Benders feasibility cut (11) must have the form of $\pi^\top x \geq \pi_0$ where $\pi \in \mathbb{R}_+^n$. Therefore, problems (4) and (15) can be written as the forms of

$$\min \{c^\top x : Cx \geq b, x \in \{0, 1\}^n\}, \quad (17)$$

$$\min \{c^\top x : Cx \geq b, x \in \{0, 1\}^n, x_j = 0, \forall j \in \mathcal{N}^0, x_j = 1, \forall j \in \mathcal{N}^1\}, \quad (18)$$

with a nonnegative constraint matrix $C \geq 0$. Since x^{LP} is a feasible solution of the LP relaxation of problem (4) (or equivalently, problem (17)), $Cx^{\text{LP}} \geq b$ and $0 \leq x^{\text{LP}} \leq 1$ must hold. Letting $\bar{x} = \lceil x^{\text{LP}} \rceil$, then $\bar{x} \in \{0, 1\}^n$ and $C\bar{x} \geq Cx^{\text{LP}} \geq b$; and by $x_j^{\text{LP}} = 0$ for $j \in \mathcal{N}^0$ and $x_j^{\text{LP}} = 1$ for $j \in \mathcal{N}^1$, we must have $\bar{x}_j = 0$ for $j \in \mathcal{N}^0$ and $\bar{x}_j = 1$ for $j \in \mathcal{N}^1$. This implies that \bar{x} is a feasible solution of problem (18), i.e., problem (15). The proof is complete. \square

Proposition 3 implies that (i) problem (4) is feasible if and only if its LP relaxation is feasible; and (ii) the RENS procedure enjoys a favorable feature, that is, it will always return a feasible solution of the original problem (4). Indeed, as will be demonstrated in Section 5.4, a high-quality feasible solution of problem (4) is usually identified by this heuristic procedure.

Although a high-quality feasible solution can potentially be found by the above heuristic procedure, our preliminary experiments showed that the computational effort spent in solving the restricted problem (15) can be large, especially when \mathcal{N}^0 and \mathcal{N}^1 are small (as the problem size is large). To save the computational effort, we enlarge the subsets \mathcal{N}^0 and \mathcal{N}^1 as

$$\mathcal{N}^0 = \{j \in [n] : x_j^{\text{LP}} \leq \theta\} \text{ and } \mathcal{N}^1 = \{j \in [n] : x_j^{\text{LP}} \geq 1 - \theta\}, \quad (19)$$

where $\theta > 0$ is a predefined value. The larger the θ , the larger the \mathcal{N}^0 and \mathcal{N}^1 are, and thus the smaller and easier the problem (15) is. In our experiments, we set $\theta = 0.01$.

4.3 MIR-enhanced Benders feasibility cuts

As mentioned in previous studies such as Bodur & Luedtke (2016); Rahmaniani et al. (2020), when constructing the Benders cuts, the BD algorithm does not consider the constraints (e.g., the integrality constraints) on variables x in the master problem. This disadvantage, however, generally leads to weak Benders cuts, resulting in weak LP relaxations and bad overall performances. To overcome this weakness, Cordeau et al. (2019) exploited the integrality requirements of x and applied the coefficient strengthening (Savelsbergh, 1994) to strengthen the Benders feasibility cuts (11). Here we explore the use of the MIR technique (Nemhauser & Wolsey, 1990; Marchand & Wolsey, 2001), which simultaneously takes the integrality and variable bound requirements of x (i.e., $x \in \{0, 1\}^n$) into consideration, to derive MIR-enhanced Benders feasibility cuts (see Bodur & Luedtke (2016) for a discussion on MIR-enhanced Benders optimality cut in the context of solving two-stage stochastic programming problems). We show that MIR-enhanced Benders feasibility cuts dominate the strengthened Benders feasibility cuts in Cordeau et al. (2019).

4.3.1 Mixed integer rounding

To proceed, we introduce the following result on the basic MIR inequality, which can be found in, e.g., (Wolsey, 2021, Proposition 8.5).

Proposition 4. *Let $b \in \mathbb{R}$ and $\mathcal{Y} = \{(x, y) \in \mathbb{Z}^1 \times \mathbb{R}_+^1 : x + y \geq b\}$. The basic MIR inequality $x + \frac{y}{f_b} \geq \lceil b \rceil$ is valid for \mathcal{Y} where $f_b = b - \lfloor b \rfloor$.*

Using Proposition 4, we can derive the MIR inequality as follows. For completeness, a proof is provided in Section 1 of the online supplement ².

Proposition 5. *Consider the set $\mathcal{X} = \{x \in \{0, 1\}^n : \sum_{j \in [n]} c_j x_j \geq b\}$. Let $(\mathcal{L}, \mathcal{U})$ be a partition of $[n]$ and $\delta > 0$. The following MIR inequality*

$$\sum_{j \in \mathcal{L}} G\left(\frac{c_j}{\delta}\right) x_j + \sum_{j \in \mathcal{U}} G\left(-\frac{c_j}{\delta}\right) (1 - x_j) \geq \lceil \beta \rceil \quad (20)$$

is valid for \mathcal{X} , where

$$\beta = \frac{b - \sum_{j \in \mathcal{U}} c_j}{\delta}, \quad G(d) = \lfloor d \rfloor + \min\left\{\frac{f_d}{f_\beta}, 1\right\}, \quad (21)$$

$$f_\beta = \beta - \lfloor \beta \rfloor, \quad f_d = d - \lfloor d \rfloor.$$

To derive the MIR-enhanced Benders feasibility cuts for formulation (4), we can present the Benders feasibility cut (11) as $\sum_{j \in [n]} c_j x_j \geq b$ where

$$c_j = \sum_{\omega \in [s], A_i^\omega \bar{x} \leq 1} p_i^\omega a_{ij}^\omega, \quad j \in [n], \quad \text{and } b = 1 - \epsilon_i - \sum_{\omega \in [s], A_i^\omega \bar{x} > 1} p_i^\omega, \quad (22)$$

select the partition $(\mathcal{L}, \mathcal{U})$ of $[n]$ and parameter $\delta > 0$, and apply Proposition 5 to construct the resultant inequality (20). In order to possibly find an inequality violated by a given vector $\bar{x} \in [0, 1]^n$, we choose the partition $(\mathcal{L}, \mathcal{U})$ of $[n]$ and parameter $\delta > 0$ using the following heuristic procedure. The partition $(\mathcal{L}, \mathcal{U})$ of $[n]$ is set to $\mathcal{L} = \{j \in [n] : \bar{x}_j < \frac{1}{2}\}$ and $\mathcal{U} = \{j \in [n] : \bar{x}_j \geq \frac{1}{2}\}$. As for

²The online supplement is available at https://drive.google.com/file/d/1Cu_BmYsw6tpppf0yxCaUwBbt2ru83MzK/view?usp=sharing.

parameter δ , we take the values in $\mathcal{F} = \{[c_j] : c_j \neq 0, 0 < \bar{x}_j < 1, j \in [n]\}$. We construct the MIR inequalities for all $\delta \in \mathcal{F}$, and choose the one with the greatest violation. Here the violation of an inequality $\sum_{j \in [n]} \pi_j x_j \geq \pi_0$ at a point \bar{x} is defined as $\frac{\max\{\pi_0 - \sum_{j \in [n]} \pi_j \bar{x}_j, 0\}}{\|\pi\|}$, where $\|\cdot\|$ denotes the Euclidean norm. A similar heuristic procedure has been used by Marchand & Wolsey (2001) to construct violated \leq -MIR inequalities for the set $\{x \in \mathbb{R}^p \times \mathbb{Z}^{n-p} : \sum_{j \in [n]} c_j x_j \leq b, \ell \leq x \leq u\}$.

4.3.2 Comparison with the strengthened Benders feasibility cut in Cordeau et al. (2019)

Next, we illustrate the strength of the MIR-enhanced Benders feasibility cut (20) for formulation (4) by comparing it with the strengthened Benders feasibility cut in Cordeau et al. (2019).

We first introduce the strengthened Benders feasibility cut. Without loss of generality, we assume $b > 0$ where b is defined in (22), as otherwise, $\mathcal{X} = \{0, 1\}^n$ and no violated inequality can be derived from \mathcal{X} . In addition, from the definitions of c_j and b in (22), $p_i^\omega > 0$, $\sum_{\omega \in [s]} p_i^\omega = 1$, $\epsilon_i > 0$, and $a_{ij}^\omega \in \{0, 1\}$, we must have

Observation 6. *Let c_j and b be defined as in (22). Then $0 \leq c_j \leq 1$ for all $j \in [n]$ and $0 < b < 1$.*

Using the integrality and nonnegativity of variables x_j , Cordeau et al. (2019) modified the coefficient c_j to $\min\{c_j, b\}$ in the Benders feasibility cut $\sum_{j \in [n]} c_j x_j \geq b$ and derived the strengthened Benders feasibility cut

$$\sum_{j \in [n]} \min\{c_j, b\} x_j \geq b. \quad (23)$$

Proposition 7. *The strengthened Benders feasibility cut (23) is equivalent to the MIR-enhanced Benders feasibility cut (20) with $\mathcal{L} = [n]$, $\mathcal{U} = \emptyset$, and $\delta = 1$.*

Proof. Suppose that $\mathcal{L} = [n]$, $\mathcal{U} = \emptyset$, and $\delta = 1$. By (21) and Observation 6, we have $G(c_j) = [c_j] + \min\left\{\frac{f_{c_j}}{f_b}, 1\right\} = [c_j] + \min\left\{\frac{c_j - [c_j]}{b - [b]}, 1\right\}$. If $c_j = 1$, then $G(c_j) = 1 = \min\left\{\frac{c_j}{b}, 1\right\}$; otherwise, $G(c_j) = \min\left\{\frac{c_j}{b}, 1\right\}$. Together with $[\beta] = [b] = 1$, this indicates that (23) is a scalar multiple of (20) with the scalar being b . As a result, inequalities (20) and (23) are equivalent. \square

Under certain conditions, the MIR-enhanced Benders feasibility cut (20) can be stronger than the strengthened Benders feasibility cut (23).

Proposition 8. *Let $\mathcal{S} = \{j \in [n] : c_j \geq b\}$. If $0 < \sum_{j \in [n] \setminus \mathcal{S}} c_j < b$, then the MIR inequality (20) with $\mathcal{L} = \mathcal{S}$, $\mathcal{U} = [n] \setminus \mathcal{S}$, and $\delta = 1$ reduces to*

$$\sum_{j \in \mathcal{S}} x_j \geq 1, \quad (24)$$

which is stronger than the strengthened Benders feasibility cut (23).

Proof. Suppose that $\mathcal{L} = \mathcal{S}$, $\mathcal{U} = [n] \setminus \mathcal{S}$, $\delta = 1$. Then from (21), Observation 6, and $\sum_{j \in [n] \setminus \mathcal{S}} c_j < b$, we have $[\beta] = [b - \sum_{j \in [n] \setminus \mathcal{S}} c_j] = 1$ and $f_\beta = b - \sum_{j \in [n] \setminus \mathcal{S}} c_j$. For $j \in \mathcal{S}$, if $c_j = 1$, it follows $G(c_j) = [c_j] + \min\left\{\frac{f_{c_j}}{f_\beta}, 1\right\} = 1$; otherwise, it also follows $f_{c_j} = c_j$ and $G(c_j) = [c_j] + \min\left\{\frac{f_{c_j}}{f_\beta}, 1\right\} = \min\left\{\frac{c_j}{b - \sum_{j' \in [n] \setminus \mathcal{S}} c_{j'}}, 1\right\} = 1$. For $j \in [n] \setminus \mathcal{S}$, if $c_j = 0$, it follows $G(-c_j) = [-c_j] + \min\left\{\frac{f_{-c_j}}{f_\beta}, 1\right\} = 0$;

otherwise, $f_{-c_j} = 1 - c_j > 0$ and $G(-c_j) = \lfloor -c_j \rfloor + \min \left\{ \frac{f_{-c_j}}{f_\beta}, 1 \right\} = -1 + \min \left\{ \frac{1 - c_j}{b - \sum_{j' \in [n] \setminus \mathcal{S}} c_{j'}}, 1 \right\} = 0$. Thus, (20) reduces to (24). By $\sum_{j \in [n]} \min\{c_j, b\}x_j = b \sum_{j \in \mathcal{S}} x_j + \sum_{j \in [n] \setminus \mathcal{S}} c_j x_j \geq b \sum_{j \in \mathcal{S}} x_j$, (24) must be stronger than (23). \square

Propositions 7 and 8 demonstrate that by choosing appropriate $(\mathcal{L}, \mathcal{U})$ and δ , we can obtain an MIR-enhanced Benders feasibility cut (20) that is either identical to or stronger than the strengthened Benders feasibility cut (23) (under certain conditions). This shows the potential of the MIR-enhanced Benders feasibility cut in strengthening the LP relaxation of formulation (4). In Section 5.4, we will further demonstrate this by numerical experiments.

5 Numerical results

In this section, we present the computational results to show the effectiveness and efficiency of the proposed BD algorithm and enhancement techniques for the PSCP. To do this, we first perform experiments on small-scale PSCP instances to demonstrate the advantage of the proposed BD algorithm over state-of-the-art MIP solvers. Then, we present detailed computational results of the proposed BD algorithm on large-scale PSCP instances. Finally, we evaluate the performance impact of the enhancement techniques developed in Section 4 for the PSCP³.

The proposed BD algorithm was implemented in Julia 1.7.3 using CPLEX 20.1.0. We set parameters of CPLEX to run the code in a single-threaded mode, with a time limit of 7200 seconds and a relative MIP gap tolerance of 0%. Unless otherwise specified, other parameters in CPLEX were set to their default values. All computational experiments were performed on a cluster of Intel(R) Xeon(R) Gold 6140 CPU @ 2.30GHz computers.

5.1 Testsets

In our experiments, we construct the PSCP instances using the 60 deterministic SCP instances with up to 500 rows and 5000 columns, as considered in Fischetti & Monaci (2012). These instances are publicly available at the ORLIB library⁴. We use two different distributions of random vectors A_i to construct the scenarios (vectors) A_i^ω for the PSCP instances. In the first case, each a_{ij} is assumed to be an independent Bernoulli random variable (Hwang, 2004; Fischetti & Monaci, 2012). Specifically, for a constraint matrix A of a deterministic SCP instance, each a_{ij} , $j \in \text{supp}(A_i)$, has a probability p_{ij} to be disappeared, randomly chosen from $[0, 0.4]$, and each $j \in [n] \setminus \text{supp}(A_i)$ has a probability 1 to be disappeared. In the second case, each row (a_{i1}, \dots, a_{in}) is assumed to be conditionally independent, following the Bernoulli mixture distribution considered in Ahmed & Papageorgiou (2013) (and thus random variables a_{ij_1} and a_{ij_2} can be correlated). In particular, given a finite prior distribution $\{\pi_1, \dots, \pi_L\}$, the conditional probabilities $p_{ij_1\ell}$ and $p_{ij_2\ell}$ (corresponding to the disappearance of columns j_1 and j_2 in scenario ℓ) are independent for $j_1, j_2 \in [n]$ with $j_1 \neq j_2$ and $\ell \in [L]$. In our experiments, L is set to 50; each π_ℓ is uniformly chosen from $[0, 1]$ and normalized such that $\sum_{\ell=1}^L \pi_\ell = 1$; and similar to the independent case, $p_{ij\ell}$, $j \in \text{supp}(A_i)$, are uniformly chosen from $[0, 0.4]$, and $p_{ij\ell}$, $j \in [n] \setminus \text{supp}(A_i)$, are set to 1.

We construct the PSCP instances based on the above two independent and correlated distributions of random vectors A_i , and the instances are thus referred as to independent and correlated

³In Section 2 of the online supplement, we present the computational results to compare the proposed BD algorithm with the state-of-the-art approach in Jiang & Xie (2022) on the PSCP with $m = 1$.

⁴<http://people.brunel.ac.uk/~mastjjb/jeb/orlib/scpinfo.html>

instances, respectively. The first testset T_1 consists of small-scale instances in which s is set to 100 and $\epsilon_i, i \in [m]$, are set to the common value ϵ , chosen from $\{0.05, 0.1\}$. The second testset T_2 consists of large-scale instances in which s is chosen from $\{1000, 2000\}$ and similarly, $\epsilon_i, i \in [m]$, are set to the common value ϵ , chosen from $\{0.025, 0.05, 0.1\}$. In total, there are 240 and 720 instances in testsets T_1 and T_2 , respectively. It deserves to mention that in all constructed instances, condition (13) does not hold for all $i \in [m]$, and thus all constructed instances are feasible.

5.2 Comparison with state-of-the-art MIP solvers

In this subsection, we show the advantage of the proposed BD algorithm for the PSCP based on formulation (4) over the direct use of CPLEX applied as a black-box MIP solver to formulation (2). To do this, we compare the following settings:

- **CPX**: formulation (2) is solved using CPLEX's branch-and-cut solver;
- **AUTO-BD**: formulation (2) is solved using CPLEX's automatic BD algorithm (by setting parameter "Benders strategy" to "full");
- **BD**: formulation (4) is solved using the proposed BD algorithm in which the Benders feasibility cuts are separated for integer and fractional solutions at all nodes of the search tree;
- **RBD**: formulation (4) is solved using the proposed BD algorithm in which the Benders feasibility cuts are separated for integer solutions at all nodes and fractional solutions at the root node of the search tree.

Notice that (i) in settings **CPX** and **AUTO-BD**, the integrality constraints (2d) in formulation (2) are (equivalently) relaxed into $0 \leq z_i^\omega \leq 1$ for $i \in [m]$ and $\omega \in [s]$; and (ii) in settings **BD** and **RBD**, the three enhancement techniques (i.e., initial cuts, the customized RENS heuristic algorithm, and the MIR-enhanced Benders feasibility cuts) in Section 4 are all implemented.

Figures 1a and 1b give the performance profiles comparing the CPU times and the end gaps (when the time limit was hit) returned by settings **CPX**, **AUTO-BD**, **BD**, and **RBD**. Detailed statistics of instance-wise computational results can be found in Tables 1 to 4 in the Appendix. First, from Figures 1a and 1b, we can conclude that the performances of the proposed **BD** and **RBD** are fairly comparable on the small-scale instances in testset T_1 . Overall, **RBD** seems to perform slightly better than **BD** on easy instances. Second, we observe from the two figures that the proposed **BD** and **RBD** outperform **CPX** by at least one order of magnitude. In particular, as demonstrated in Figure 1a, almost all instances can be solved by **BD** and **RBD** within the time limit, while less than 50% of the instances can be solved by **CPX**. For the unsolved instances, the end gap returned by **CPX** is also much larger than those returned by **BD** and **RBD**, as shown in Figure 1b. Finally, we observe that **AUTO-BD** also performs fairly well. In particular, **AUTO-BD** can also solve most instances to optimality within the time limit. This may be explained by the reason that the main difference between our proposed **BD/RBD** and **AUTO-BD** lies in the way to solve the Benders subproblem (5) to obtain the Benders feasibility cut (8), and according to Bonami et al. (2020), the Benders subproblem (5) may also be efficiently solved by **AUTO-BD** with the technique to handle the so-called *generalized bound constraints* (2a). Nevertheless, we observe that **AUTO-BD** is outperformed by the proposed **BD** and **RBD**, especially for the easy instances. In particular, more than 50% of the instances can be solved within 10 seconds by the proposed **BD** and **RBD** while only about 35% of the instances can be solved within 10 seconds by **AUTO-BD**.

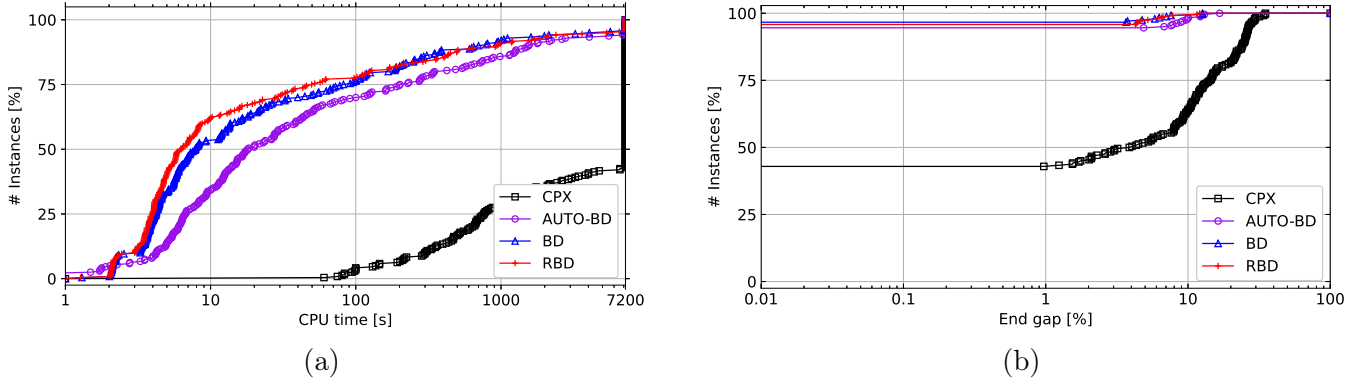


Figure 1: Performance profiles of the CPU times and end gaps on the instances in testset T_1 .

5.3 Computational results on large-scale instances

We now evaluate the performances of the proposed BD and RBD on the large-scale instances in testset T_2 . Figure 2 summarizes the computational results, grouped by ϵ , s , and the type of instances (i.e., independent or correlated instances). Detailed statistics of instance-wise computational results can be found in Tables 2-13 of the online supplement.

First, we can observe from Figures 2a and 2b that the PSCP instances with $\epsilon = 0.025$ are much more difficult to be solved by BD and RBD compared with those with $\epsilon = 0.05, 0.1$. Specifically, for instances with $\epsilon = 0.05, 0.1$, RBD and BD can solve all of them to optimality while for instances with $\epsilon = 0.025$, RBD and BD were only able to solve about 15% and 35% of the instances to optimality, respectively. The reason can be explained as follows. The PSCP instances with $\epsilon = 0.025$ are much more constrained than those with $\epsilon = 0.05, 0.1$, which not only leads to a weak LP bound at the root node but also makes BD and RBD challenging to find optimal or near-optimal solutions. To justify this, we present the performance profiles of the root gaps of the LP bound at the root node and the primal gaps of the solution (for instances with $\epsilon = 0.025$) returned by BD and RBD in Figures 3a and 3b, respectively. The root gap and primal gap of an instance are computed as $100 \times \frac{o^* - o_{\text{root}}}{o^*}$ and $100 \times \frac{o^F - o^*}{o^*}$, respectively, where o^* , o_{root} , and o^F are the optimal value or the best incumbent⁵, the LP bound obtained at the root node, and the objective value of the feasible solution returned by BD/RBD, respectively. As shown in Figures 3a and 3b, (i) the root gaps of instances with $\epsilon = 0.025$ are much larger than those of instances with $\epsilon = 0.05, 0.1$; and (ii) the primal gaps of instances with $\epsilon = 0.025$ are fairly large, which confirms our statement. It is worthy noting that the different quality of the LP bounds also makes the different performance behavior of the proposed BD and RBD on instances with different ϵ . Overall, we observe that for instances with $\epsilon = 0.05, 0.1$, RBD performs better than BD, while for those with $\epsilon = 0.025$, BD performs much better. This is reasonable as instances with $\epsilon = 0.025$ generally associate with a weak LP bound (as shown in Figure 3a), and the strategy of adding cuts for fractional solutions encountered in the whole search tree in BD can strengthen the lower bound more quickly, and thus makes the performance of BD better than that of RBD. For instances with $\epsilon = 0.05, 0.1$ that generally associate with a relatively good LP bound, the same strategy cannot compensate for the additional overhead of making a large LP relaxation (as more cuts are added), and thus makes the performance of BD worse than that of RBD.

Next, we compare the results of the PSCP instances with different numbers of scenarios s .

⁵For an unsolved instance by BD and RBD with a 7200 seconds time limit, the best incumbent o^* is obtained by solving it using BD with a 36000 seconds time limit. Note that BD performs better than RBD on hard instances with $\epsilon = 0.025$, as shown in Figure 2b.

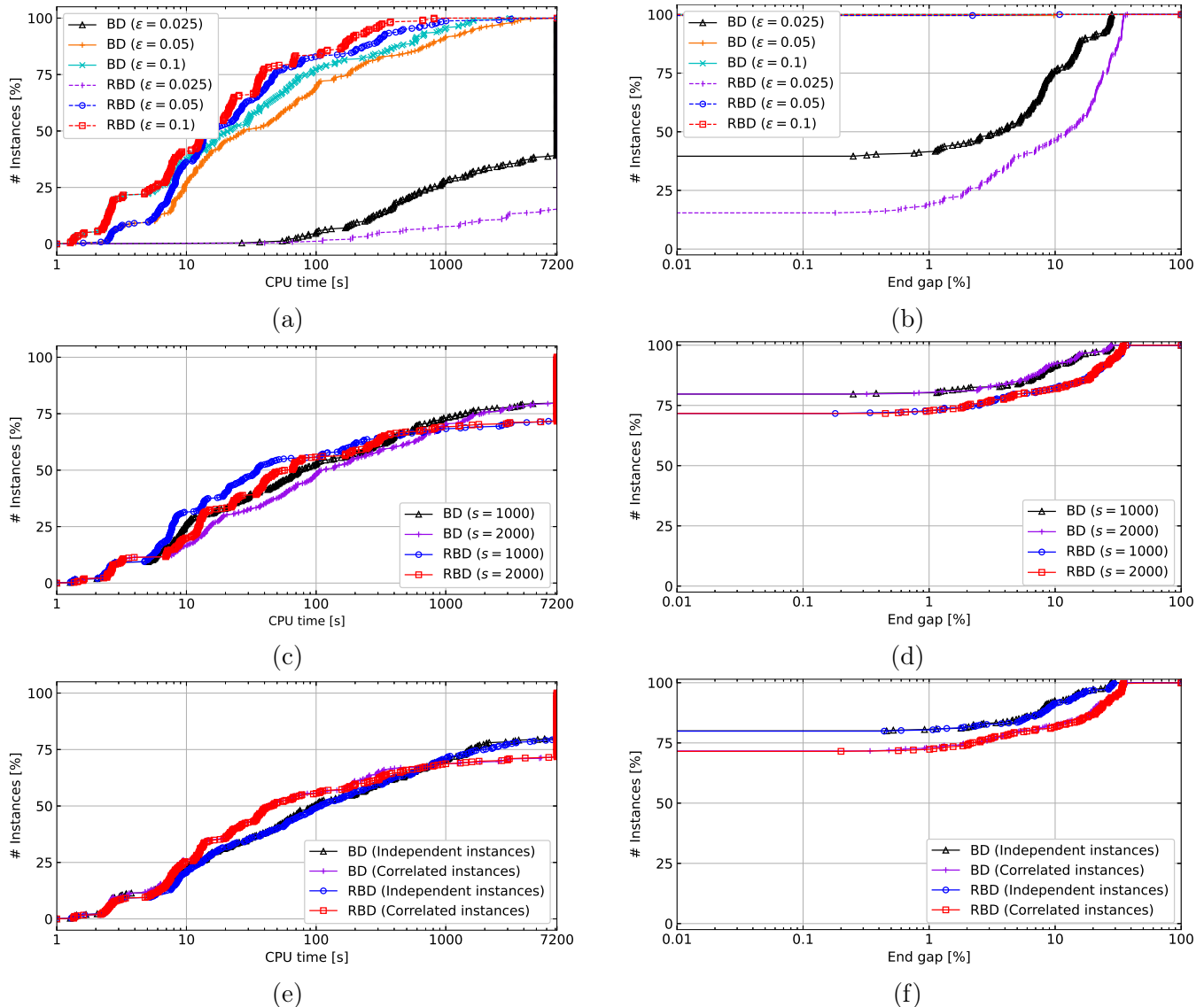


Figure 2: Performance profiles of the CPU times and end gaps on the instances in testset T_2 . (a) and (b): grouped by ϵ ; (c) and (d): grouped by s ; (e) and (f): grouped by independent and correlated instances.

Figures 2c and 2d show that solving instances with $s = 2000$ by BD and RBD is only slightly more difficult than solving those with $s = 1000$. This is due to the reasons that (i) for the PSCP instances with different s , the numbers of variables in (4) are identical; and (ii) for the proposed BD or RBD, the main difference in solving the PSCP instances with different s lies in how fast we obtain the Benders feasibility cuts (11), and as demonstrated in Section 3.2, the Benders feasibility cuts (11) can be computed by an efficient polynomial-time algorithm. Indeed, in our experiments, we observed that the overhead spent in the computations of the Benders feasibility cuts (11) is not large, especially for the RBD. These results highlight the scalability of the proposed BD and RBD in solving large-scale PSCP instances (with large numbers of scenarios).

Finally, we observe from Figures 2e and 2f that the performances of BD and RBD on the independent and correlated PSCP instances are quite similar. This is reasonable knowing that (i) our proposed BD and RBD for the PSCP do not require a specific distribution of the random data A_i ; and (ii) the independent and correlated distributions of A_i that are used to construct the scenarios A_i^ω are quite similar (indeed, the independent distribution of A_i can be seen as a special case of the correlated

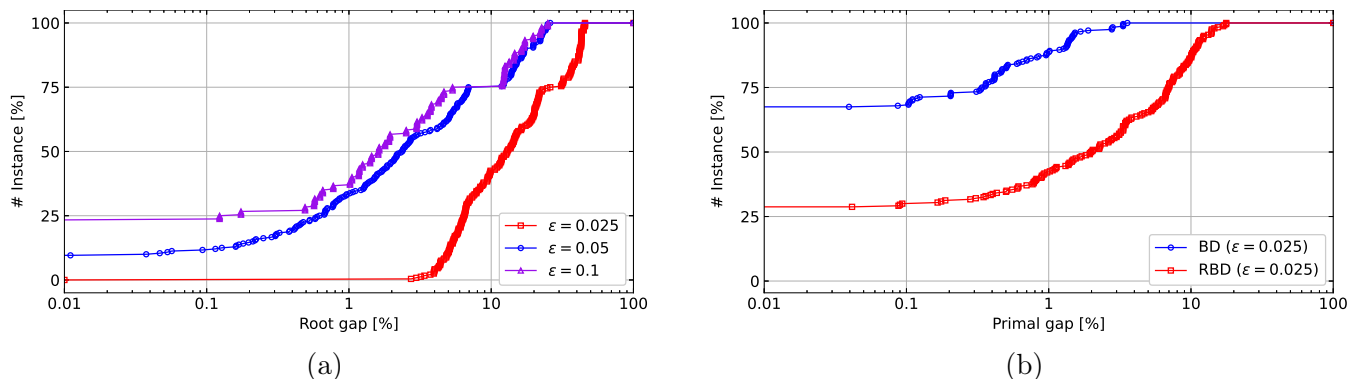


Figure 3: (a) Performance profiles of the root gaps on the instances in testset T_2 ; (b) Performance profiles of the primal gaps on the instances with $\epsilon = 0.025$ in testset T_2 .

distribution of A_i with $L = 1$).

5.4 Performance effects of the three enhancement techniques in Section 4

In this subsection, we evaluate the performance effects of the three enhancement techniques (i.e., initial cuts, the customized RENS heuristic algorithm, and the MIR-enhanced Benders feasibility cuts) in Section 4 for solving the PSCP. To do this, we compare the following variants of setting BD:

- **BasicBD**: the basic version of setting BD in which none of the three techniques is implemented;
- **BasicBD+IC**: the setting **BasicBD** together with the initial cuts proposed in Section 4.1;
- **BasicBD+IC+H**: the setting **BasicBD+IC** together with the customized RENS heuristic algorithm proposed in Section 4.2;
- **BasicBD+IC+H+MIR**: the setting **BasicBD+IC+H** together with the MIR-enhanced Benders feasibility cuts proposed in Section 4.3, i.e., setting BD.

We do not compare the corresponding variants of RBD as our preliminary experiments showed that the obtained results are similar to those presented in this subsection. Figure 4 displays the performance profiles of the CPU times, end gaps, root gaps, and number of explored nodes on the instances in testset T_2 returned by the four settings. Detailed statistics of instance-wise computational results can be found in Tables 14-25 of the online supplement.

First, we can observe from Figure 4a that compared with those returned by **BasicBD**, the number of solved instances returned by **BasicBD+IC** is much larger and the CPU time returned by **BasicBD+IC** is much smaller. The reason can be seen in Figures 4c and 4d in which we observe that with the initial cuts (14), **BasicBD+IC** can return a much better root gap and a much smaller number of explored nodes than **BasicBD**. This shows that initial cuts (14) can indeed strengthen the LP relaxation of formulation (4) (as they enable CPLEX to construct further internal cuts) and thus improve the overall performance of the proposed BD algorithm.

Next, we evaluate the performance effect of the customized RENS heuristic algorithm in Section 4.2. Comparing **BasicBD+IC** and **BasicBD+IC+H** in Figures 4a and 4b, we find that although the customized RENS heuristic algorithm does not contribute to increase the number of solved instances and reduce the overall solution time of the solved instances, it can effectively reduce the end gap of the unsolved instances. To gain deeper insight into the computational efficiency of the customized RENS heuristic algorithm, we report the primal gaps of the solutions returned by the

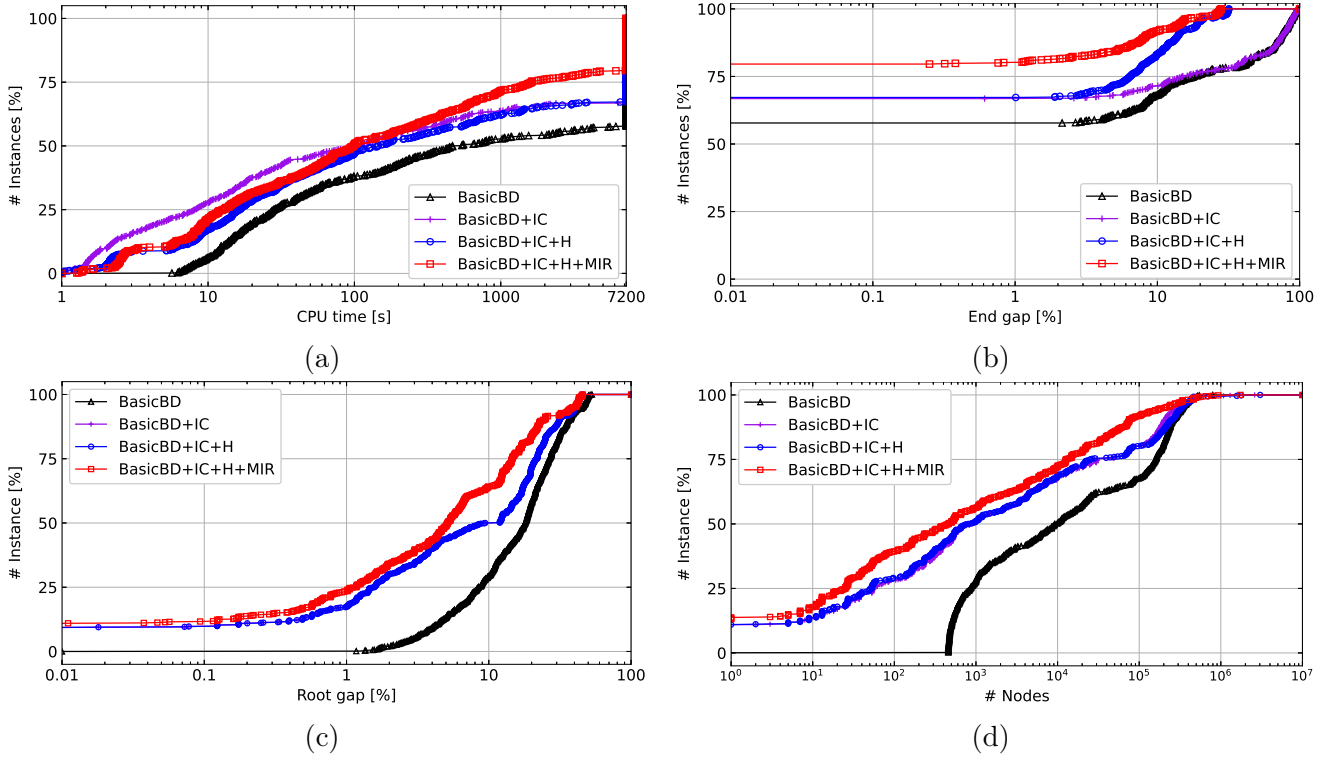


Figure 4: Performance profiles of the CPU times, end gaps, root gaps, and number of explored nodes on the instances in testset T_2 .

customized RENS heuristic algorithm in Figure 5. As shown in Figure 5, for about 75% of the instances, the primal gap of the solutions returned by `BasicBD+IC+H` is less than 1%, which highlights the effectiveness of the customized RENS heuristic algorithm in providing a high-quality solution for the PSCP and improving the overall performance of the BD algorithm on the hard instances.

Finally, we evaluate the performance effect of the MIR-enhanced Benders feasibility cuts in Section 4.3. As shown in Figure 4c, with the MIR-enhanced Benders feasibility cuts, the root gap returned by `BasicBD+IC+H+MIR` is much smaller than that returned by `BasicBD+IC+H`, which shows the effectiveness of the MIR-enhanced Benders feasibility cuts in strengthening the LP relaxation of formulation (4). As a result, equipped with the MIR-enhanced Benders feasibility cuts, the proposed BD algorithm performs much better. In particular, the number of explored nodes and the CPU time (of the hard instances) returned by `BasicBD+IC+H+MIR` are much smaller, and more than 10% instances can be solved to optimality with the time limit.

In summary, our results show that the three enhancement techniques presented in Section 4 can all improve the overall performance of the BD algorithm in terms of achieving a better solution time or a better end gap.

6 Conclusions and future works

In this paper, we consider the PSCP in which each row of the constraint matrix is a Bernoulli random vector and has a finite discrete distribution. We develop an efficient BD algorithm based on a Benders reformulation of the PSCP. Two key features of the proposed BD algorithm, which make it particularly suitable to solve large-scale PSCPs, are: (i) the number of variables in the Benders

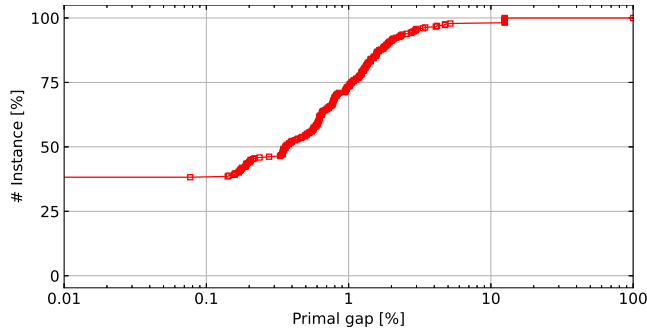


Figure 5: Performance profile of the primal gaps of the solutions returned by RENS on the instances in testset T_2 .

reformulation is equal to the number of columns but independent of the number of scenarios of the random rows; and (ii) the Benders feasibility cuts can be separated by efficient polynomial-time algorithms. We have also proposed three enhancement techniques (i.e., initial cuts, the customized RENS heuristic algorithm, and the MIR-enhanced Benders feasibility cuts) to improve the performance of the proposed BD algorithm. Extensive computational results showed that the proposed BD algorithm outperforms the state-of-the-art general-purpose MIP solver’s branch-and-cut and automatic BD algorithms. Furthermore, the proposed BD algorithm is capable of solving large-scale PSCP instances with up to 500 rows, 5000 columns, and 2000 scenarios of the random rows.

As for future work, we will develop more effective cutting planes to improve the performance of the proposed BD algorithm for solving the PSCP, especially for the case where $A_i x \geq 1$, $i \in [m]$, are required to be satisfied at a high probability $1 - \epsilon$ (e.g., $\epsilon = 0.025$). In addition, it would also be interesting to extend the proposed BD algorithm to solve the joint PSCP: $\min \{c^\top x : \mathbb{P}\{Ax \geq \mathbf{1}\} \geq 1 - \epsilon, x \in \{0, 1\}^n\}$ (Beraldi & Bruni, 2010). One difficulty of this extension is that the big-M reformulation of the joint PSCP provides a very weak LP relaxation bound, hindering the convergence of the BD algorithm; see Section 4 of the online supplement for more details. In order to develop an efficient BD algorithm for solving the joint PSCP, we need to develop effective cutting planes (by judiciously exploiting the special structure of the problem) to strengthen the big-M reformulation of the joint PSCP.

Acknowledgement

We would like to thank the two anonymous reviewers for their insightful comments. Jie Liang, Cheng-Yang Yu, and Wei Lv contributed equally and are joint first authors. The work of Wei-Kun Chen was supported in part by the Chinese NSF grants (No. 12101048). The work of Yu-Hong Dai was supported in part by the Chinese NSF grants (Nos. 12021001 and 11991021).

Appendix. Detailed computational results

Table 1: Performance comparison of settings CPX, AUTO-BD, BD, and RBD for the independent instances with $\epsilon = 0.05$ in testset T_1 . T (G %) denotes that the CPU time is T if the instance is solved within the timelimit; otherwise, it denotes that the end gap returned by CPLEX is G %. N denotes the number of explored nodes.

Name	CPX		AUTO-BD		BD		RBD	
	T (G %)	N	T (G %)	N	T (G %)	N	T (G %)	N
scp41	516.0	1298	6.2	236	4.5	22	4.2	86
scp42	675.3	1563	8.3	542	4.3	53	4.3	464
scp43	411.7	1163	6.9	595	4.2	58	4.1	155
scp44	60.3	11	4.5	0	3.6	5	3.5	4
scp45	208.6	581	4.9	35	3.5	5	3.5	5
scp46	82.5	35	6.4	18	3.8	7	3.5	7
scp47	94.6	120	5.6	84	3.6	7	3.6	11
scp48	95.8	47	5.2	83	3.7	9	3.7	12
scp49	1191.5	3401	11.2	2050	6.0	312	5.4	1263
scp410	288.3	668	7.9	378	4.5	46	4.4	251
scp51	365.2	805	12.1	715	5.4	97	4.5	280
scp52	1389.3	4284	13.5	801	5.7	82	4.8	311
scp53	1306.2	3955	13.9	643	6.0	115	5.1	597
scp54	1342.3	4891	14.9	1340	6.0	103	4.9	454
scp55	72.5	51	8.1	0	3.8	7	3.8	9
scp56	150.1	165	9.6	54	4.2	13	4.2	23
scp57	354.8	881	12.0	186	5.0	52	4.5	137
scp58	1216.5	5037	12.5	1224	6.7	236	5.0	614
scp59	223.2	329	13.0	159	4.7	35	4.3	70
scp510	2034.8	6250	14.2	921	5.8	125	5.6	987
scp61	4401.4	19537	11.1	2240	6.7	457	7.0	1823
scp62	1552.1	6165	8.6	1868	5.7	195	5.9	1351
scp63	397.5	1446	5.2	667	4.5	53	4.1	186
scp64	311.3	897	6.7	314	4.6	37	4.2	156
scp65	(5.2)	13594	68.7	16238	23.2	4308	36.5	21956
scpa1	(4.5)	4800	124.8	10244	43.3	3118	32.3	8631
scpa2	(1.5)	7649	114.9	6831	14.4	434	16.4	4191
scpa3	(2.1)	6229	38.7	1683	8.3	127	8.3	1605
scpa4	(3.0)	5964	45.5	2802	11.8	529	11.8	2197
scpa5	(2.0)	5710	51.4	3960	11.4	352	9.7	1743
scpb1	(11.4)	5594	335.2	31402	87.5	12834	122.3	57770
scpb2	(11.7)	6661	576.6	95526	193.1	25416	190.0	98827
scpb3	(11.5)	4869	341.4	25726	90.1	10854	97.1	43021
scpb4	(13.1)	4553	720.0	96625	193.2	24709	246.3	153084
scpb5	(10.8)	4727	233.7	18253	47.4	3834	48.8	23480
scpc1	(8.6)	2202	573.7	32800	73.1	3829	115.4	30432
scpc2	(8.2)	1759	881.5	69243	351.4	29043	358.2	113709
scpc3	(9.1)	1423	2262.3	312112	778.3	75759	1829.2	501243
scpc4	(5.7)	2021	276.6	8374	36.6	2050	27.9	4645
scpc5	(9.0)	2337	1103.1	102990	166.2	15332	304.1	97395
scpd1	(13.7)	2664	652.8	41611	110.0	9014	108.9	34953
scpd2	(13.3)	2874	1452.5	154692	317.9	51405	437.0	226652
scpd3	(14.6)	2509	4063.0	714490	1092.1	186792	1624.0	804046
scpd4	(15.6)	2833	1553.4	163159	448.7	53332	953.9	477418
scpd5	(14.5)	2595	1236.6	128150	311.0	36591	413.3	200392
scpe1	(23.8)	202909	291.9	440769	20.0	8267	997.0	1209582
scpe2	(14.9)	124022	23.0	39773	20.9	7898	13.8	20017
scpe3	(17.3)	143209	28.0	44787	27.8	11285	22.8	36916
scpe4	(15.5)	244409	72.1	137334	569.5	182845	408.8	473928
scpe5	(12.8)	127191	21.7	35065	26.9	11054	15.8	25085
scpnre1	(23.7)	1887	(9.9)	618781	(3.3)	841592	(4.4)	2918483
scpnre2	(26.7)	1515	(8.9)	2117769	(6.2)	739139	(6.5)	2888883
scpnre3	(28.0)	1802	(10.1)	646693	3546.1	507681	6513.6	3802223
scpnre4	(22.6)	2335	(9.7)	600269	(4.7)	904683	(5.2)	3131983
scpnre5	(24.1)	1669	(4.9)	2802269	3531.8	490633	(4.6)	3309083
scpnrf1	(29.5)	1623	(12.2)	806303	1543.4	258465	2083.0	1524626
scpnrf2	(25.4)	3631	1385.3	946283	787.9	131735	940.8	878851
scpnrf3	(28.8)	2385	5485.7	2478715	2063.2	330887	2048.9	1414203
scpnrf4	(28.5)	2111	6998.8	2677316	5211.1	948167	(4.6)	5155605
scpnrf5	(34.9)	2431	(16.7)	2504969	(11.1)	804432	(11.6)	2339715

Table 2: Performance comparison of settings CPX, AUTO-BD, BD, and RBD for the independent instances with $\epsilon = 0.1$ in testset T_1 . T (G %) denotes that the CPU time is T if the instance is solved within the timelimit; otherwise, it denotes that the end gap returned by CPLEX is G %. N denotes the number of explored nodes.

Name	CPX		AUTO-BD		BD		RBD	
	T (G %)	N						
scp41	365.5	1663	4.2	0	2.2	0	2.2	0
scp42	293.9	1341	4.3	0	2.1	0	2.2	0
scp43	554.8	2262	6.0	71	3.5	18	3.5	21
scp44	201.3	859	1.9	0	2.1	0	2.1	0
scp45	498.2	1843	4.8	35	3.6	7	3.5	7
scp46	738.2	3436	5.5	117	3.6	24	3.4	24
scp47	133.1	253	2.0	0	1.3	0	1.3	0
scp48	722.7	3316	5.5	215	3.8	43	3.6	43
scp49	776.2	2654	5.0	31	2.1	0	2.1	0
scp410	129.7	515	4.3	0	2.1	0	2.2	0
scp51	737.7	1926	3.5	0	2.2	0	2.2	0
scp52	3180.1	19408	8.3	145	4.8	78	4.3	62
scp53	877.5	4057	9.4	43	4.1	32	3.8	32
scp54	3885.5	16160	7.3	9	4.0	5	4.0	5
scp55	95.2	147	2.8	0	2.1	0	2.2	0
scp56	624.8	2354	6.5	0	2.4	0	2.4	0
scp57	517.3	1232	6.3	0	3.6	1	3.6	1
scp58	621.5	2120	4.9	0	2.1	0	2.1	0
scp59	765.8	3024	10.5	66	4.1	16	3.7	12
scp510	1016.4	2968	4.2	0	2.1	0	2.3	0
scp61	1139.4	4046	4.3	95	3.8	30	3.7	30
scp62	2596.6	13549	5.3	122	4.0	25	3.9	25
scp63	(2.1)	11783	4.9	12	3.8	9	3.5	9
scp64	1246.2	4040	6.5	47	3.9	32	3.8	27
scp65	(2.2)	25497	5.5	807	5.5	219	4.6	218
scpa1	(5.5)	4260	14.8	413	7.9	190	5.3	204
scpa2	(1.7)	7407	12.6	347	6.0	122	4.5	130
scpa3	(2.9)	7291	15.6	275	5.6	37	4.7	37
scpa4	(1.6)	7781	15.2	110	5.4	41	4.5	38
scpa5	(4.2)	5463	15.3	79	6.1	63	4.8	47
scpb1	(9.9)	5969	31.7	7180	21.7	3125	10.3	3780
scpb2	(9.8)	5669	28.0	1336	8.1	387	5.8	365
scpb3	(11.3)	4769	18.0	1405	8.2	554	5.8	564
scpb4	(9.3)	6669	29.1	3034	12.1	1201	7.0	1435
scpb5	(6.7)	7906	20.2	622	7.3	104	5.7	117
scpc1	(7.8)	2246	38.3	2083	14.5	898	6.6	605
scpc2	(11.7)	2067	26.7	432	9.2	107	6.9	105
scpc3	(8.6)	1873	59.3	7230	43.7	4178	14.7	3839
scpc4	(8.3)	2079	23.2	443	7.5	102	5.8	158
scpc5	(8.0)	1824	54.5	2323	13.0	531	6.9	727
scpd1	(8.9)	3363	43.3	3065	13.2	973	8.4	891
scpd2	(11.2)	3615	26.3	1776	11.3	372	8.3	415
scpd3	(15.3)	2632	51.6	3287	11.5	426	8.6	857
scpd4	(12.9)	3067	39.4	5273	16.9	1640	9.5	1600
scpd5	(11.3)	3182	52.8	6557	22.0	2048	11.4	2432
scpe1	(21.7)	181178	4.6	7594	7.9	5117	7.3	8169
scpe2	1349.6	14888	1.5	479	3.5	26	3.1	32
scpe3	709.0	8289	0.7	216	3.5	60	3.0	60
scpe4	1241.4	29164	0.8	14	3.5	11	3.1	11
scpe5	(20.1)	208082	3.9	6569	3.4	19	3.0	19
scpnre1	(25.3)	1622	228.1	158928	211.4	57880	101.3	53471
scpnre2	(25.2)	1616	487.7	425608	276.5	69704	219.8	118952
scpnre3	(21.0)	1127	736.0	72439	107.3	28256	62.1	30832
scpnre4	(19.9)	2437	163.3	70287	114.1	24105	56.3	26972
scpnre5	(19.3)	1729	160.7	55359	69.4	11914	44.7	17738
scpnrf1	(28.6)	2639	197.8	84989	91.8	29188	58.9	29588
scpnrf2	(23.8)	2131	124.0	34403	66.8	14467	38.1	14502
scpnrf3	(23.5)	1671	100.4	29090	61.2	7808	33.0	8400
scpnrf4	(28.7)	2369	314.0	214797	225.7	108052	124.8	91633
scpnrf5	(30.9)	2331	794.5	671607	796.2	403883	645.3	497981

Table 3: Performance comparison of settings CPX, AUTO-BD, BD, and RBD for the correlated instances with $\epsilon = 0.05$ in testset T_1 . T (G %) denotes that the CPU time is T if the instance is solved within the timelimit; otherwise, it denotes that the end gap returned by CPLEX is G %. N denotes the number of explored nodes.

Name	CPX		AUTO-BD		BD		RBD	
	T (G %)	N	T (G %)	N	T (G %)	N	T (G %)	N
scp41	465.0	1372	6.5	434	4.3	70	4.0	212
scp42	426.0	1377	7.6	260	4.3	29	4.3	74
scp43	150.0	283	5.7	247	4.0	9	3.9	22
scp44	463.6	1813	6.0	526	4.3	98	4.1	306
scp45	504.4	1896	12.6	1619	7.1	328	5.6	1133
scp46	1221.1	2846	18.2	2796	6.0	207	7.8	1681
scp47	333.9	1366	6.0	215	4.1	31	3.9	67
scp48	483.2	1451	9.0	950	4.3	41	4.2	164
scp49	963.5	2362	11.4	938	4.3	49	4.2	164
scp410	747.3	1570	7.7	464	4.7	66	4.6	140
scp51	211.0	267	8.8	0	3.8	7	4.0	7
scp52	3402.0	13297	16.5	1058	5.8	104	5.1	788
scp53	1193.5	4214	19.9	2043	7.4	253	6.4	1570
scp54	1162.4	3870	11.4	694	5.5	105	4.9	246
scp55	84.0	59	9.4	35	4.4	8	4.2	14
scp56	304.4	657	12.9	339	5.5	43	4.3	179
scp57	768.0	2204	12.2	711	5.7	83	4.8	220
scp58	673.7	1551	16.9	693	5.5	64	4.5	121
scp59	1109.1	3464	16.5	911	6.2	79	5.2	282
scp510	852.4	2381	11.4	920	6.5	147	4.9	213
scp61	2928.7	11156	12.6	1944	6.6	270	5.6	1087
scp62	1549.5	7423	7.2	1902	5.5	235	5.4	1184
scp63	(3.1)	12542	17.1	4006	6.4	318	8.3	2397
scp64	2099.7	7740	9.3	1174	6.2	272	5.3	1016
scp65	(1.2)	16174	13.3	2992	7.0	301	7.8	2142
scpa1	(4.3)	5082	66.4	10572	38.7	2020	20.5	5354
scpa2	(4.4)	4070	92.0	8141	27.3	2072	30.6	9185
scpa3	(1.6)	6000	47.1	5355	15.1	563	13.0	2148
scpa4	(5.1)	3825	175.7	10990	26.5	1860	29.3	8787
scpa5	3848.4	5618	33.1	1288	7.9	172	6.5	514
scpb1	(12.0)	5169	731.5	131360	375.0	56091	362.4	172282
scpb2	(13.0)	4545	536.4	74148	126.5	13894	169.7	80927
scpb3	(6.6)	6614	38.8	2834	13.9	427	9.3	1315
scpb4	(8.1)	6233	57.2	10093	20.2	1146	19.8	6862
scpb5	(9.3)	5997	350.2	27663	22.6	1945	27.5	12219
scpc1	(8.0)	1637	1227.6	95782	152.6	10259	169.0	43148
scpc2	(8.1)	2014	861.1	51165	117.8	6334	171.1	40938
scpc3	(10.7)	1639	1166.2	105661	286.0	26421	427.3	134194
scpc4	(9.2)	1930	1812.1	147473	177.2	11328	446.8	119519
scpc5	(8.8)	1939	2860.1	211377	452.0	46089	493.3	133370
scpd1	(18.4)	2393	1222.4	603106	566.5	70259	1198.7	540349
scpd2	(17.2)	2703	2619.0	444077	1583.5	235201	1718.7	839856
scpd3	(11.7)	2553	2149.0	310118	556.9	74209	1181.2	558066
scpd4	(15.2)	2594	1584.3	143756	421.1	51913	289.8	119330
scpd5	(14.4)	2842	1519.5	159509	360.9	41688	499.5	173137
scpe1	(24.2)	210709	79.2	159559	232.6	89478	15.8	20447
scpe2	6559.2	135756	16.5	34516	19.1	7179	13.4	20529
scpe3	(18.3)	142223	29.0	58052	29.8	11153	21.9	36547
scpe4	3837.9	74155	9.3	17571	19.7	7596	10.2	14017
scpe5	(14.1)	114503	334.8	469452	22.4	9351	15.7	26985
scpnre1	(26.4)	1942	(7.8)	413177	3042.0	424957	3582.8	1899603
scpnre2	(26.7)	1797	(8.4)	2290269	(7.5)	652883	(7.8)	2649383
scpnre3	(24.3)	2188	(7.6)	505714	(3.7)	817621	(4.4)	3292283
scpnre4	(22.1)	2053	(9.2)	610009	(5.6)	830283	(6.1)	2890283
scpnre5	(25.4)	1271	(6.8)	2628569	6103.5	835667	(6.7)	2770183
scpnrf1	(27.3)	2431	1795.1	1116438	2516.2	590110	2399.5	2005720
scpnrf2	(22.7)	4931	1264.8	829410	1072.4	190599	902.5	802042
scpnrf3	(26.6)	3771	626.5	340005	588.7	101540	511.2	376534
scpnrf4	(33.7)	4037	(12.2)	2748769	5068.6	918957	5333.5	4163038
scpnrf5	(35.5)	2031	(13.0)	2637669	(6.1)	935515	(12.1)	2974415

Table 4: Performance comparison of settings CPX, AUTO-BD, BD, and RBD for the correlated instances with $\epsilon = 0.1$ in testset T_1 . T (G %) denotes that the CPU time is T if the instance is solved within the timelimit; otherwise, it denotes that the end gap returned by CPLEX is G %. N denotes the number of explored nodes.

Name	CPX		AUTO-BD		BD		RBD	
	T (G %)	N						
scp41	207.6	1036	6.0	31	3.6	15	3.4	15
scp42	294.9	1207	1.8	0	2.1	0	2.1	0
scp43	287.9	1433	5.9	46	3.5	3	3.3	6
scp44	469.2	1698	1.7	0	2.2	0	2.2	0
scp45	193.0	851	2.8	0	2.1	0	2.1	0
scp46	320.2	1037	3.6	0	2.2	0	2.2	0
scp47	87.8	114	1.7	0	2.1	0	2.0	0
scp48	820.9	3576	5.4	183	3.9	40	3.7	41
scp49	641.2	2470	4.0	0	2.1	0	2.1	0
scp410	102.1	171	1.8	0	2.1	0	2.1	0
scp51	595.8	1936	6.2	0	2.2	0	2.3	0
scp52	(2.0)	26268	6.7	185	5.0	91	4.3	136
scp53	650.3	2532	8.3	0	2.5	0	2.4	0
scp54	3098.5	16503	9.5	23	4.1	35	3.8	40
scp55	97.6	122	2.2	0	2.2	0	2.1	0
scp56	682.2	3019	6.2	0	2.2	0	2.1	0
scp57	611.2	2358	10.8	71	4.5	25	4.1	27
scp58	455.2	1861	3.4	0	2.2	0	2.3	0
scp59	962.9	3309	10.2	62	4.4	68	3.9	70
scp510	836.6	2338	9.9	5	3.9	7	3.8	7
scp61	2137.2	11661	5.7	255	4.7	176	4.1	122
scp62	2539.5	9760	6.8	108	4.0	40	3.8	44
scp63	1743.8	4370	5.2	15	3.6	9	3.6	9
scp64	2575.1	11502	6.3	34	3.8	19	3.8	19
scp65	(1.6)	24010	6.8	639	5.0	174	4.3	243
scpa1	(3.1)	5831	14.0	682	7.1	196	5.1	214
scpa2	(2.4)	7493	15.0	121	5.7	40	4.9	51
scpa3	(4.5)	6633	14.8	253	6.0	46	4.9	36
scpa4	(5.5)	5530	17.2	267	6.7	144	5.0	71
scpa5	(1.7)	8369	12.5	71	4.9	21	4.6	23
scpb1	(13.2)	5298	29.2	6610	20.0	3247	8.3	3072
scpb2	(12.3)	4569	27.6	885	6.9	86	5.8	219
scpb3	(10.6)	5909	27.4	2604	11.0	1355	5.8	671
scpb4	(9.9)	6605	30.6	1522	12.8	1098	6.3	960
scpb5	(9.7)	6669	19.7	826	8.6	412	6.5	476
scpc1	(8.0)	2127	43.8	2236	12.5	447	7.8	676
scpc2	(6.0)	2238	49.1	2364	18.9	1177	7.3	1116
scpc3	(10.7)	1887	81.8	14341	63.1	8151	22.5	7361
scpc4	(7.9)	1558	26.5	528	8.2	157	5.9	122
scpc5	(8.6)	2275	44.5	2707	16.2	1396	7.1	1049
scpd1	(12.7)	3049	24.2	1121	12.5	595	7.7	514
scpd2	(13.2)	2915	41.5	4893	11.3	317	8.0	270
scpd3	(11.1)	2531	33.6	2068	13.3	812	8.5	874
scpd4	(14.2)	2633	51.6	7123	18.5	1183	9.7	1406
scpd5	(12.5)	2877	41.3	2717	15.7	1063	8.5	730
scpe1	(22.0)	165023	4.0	6056	7.8	5758	6.2	6113
scpe2	628.0	6694	0.7	75	3.3	36	3.1	27
scpe3	6625.8	194620	0.7	158	3.4	78	3.1	93
scpe4	4854.2	162737	0.8	18	3.3	16	3.2	16
scpe5	(21.4)	175247	20.4	39241	11.7	9544	17.5	27729
scpnre1	(25.5)	1482	272.4	167386	165.8	53354	111.4	65132
scpnre2	(25.6)	1322	421.6	306212	256.4	92581	206.5	123987
scpnre3	(20.7)	2141	190.4	99597	115.6	26685	62.0	31303
scpnre4	(26.5)	1739	159.5	59464	107.0	22704	46.5	19717
scpnre5	(20.9)	1492	129.1	70924	81.1	15504	42.4	15901
scpnrf1	(26.6)	1703	201.3	78791	93.8	25706	52.5	24857
scpnrf2	(22.9)	2625	282.1	31782	54.4	12568	38.9	12146
scpnrf3	(23.2)	1591	123.9	24673	56.3	8625	33.6	7180
scpnrf4	(29.4)	2248	282.8	161728	185.8	75329	128.6	88579
scpnrf5	(26.1)	3425	991.6	969952	793.0	481697	600.5	480505

References

- Ahmed, S., & Papageorgiou, D. J. (2013). Probabilistic set covering with correlations. *Operations Research*, *61*, 438–452.
- Ahmed, S., & Shapiro, A. (2008). Solving chance-constrained stochastic programs via sampling and integer programming. In *State-of-the-Art Decision-Making Tools in the Information-Intensive Age* (pp. 261–269).
- Azizi, N., García, S., & Irawan, C. A. (2022). Discrete location problems with uncertainty. In S. Salhi, & J. Boylan (Eds.), *The Palgrave Handbook of Operations Research* (pp. 43–71).
- Ben-Tal, A., Nemirovski, A., & El Ghaoui, L. (2009). *Robust Optimization*. Princeton Series in Applied Mathematics. Princeton University Press, New Jersey.
- Beraldi, P., & Bruni, M. E. (2010). An exact approach for solving integer problems under probabilistic constraints with random technology matrix. *Annals of Operations Research*, *177*, 127–137.
- Beraldi, P., & Ruszczyński, A. (2002). The probabilistic set-covering problem. *Operations Research*, *50*, 956–967.
- Berthold, T. (2014). RENS: the optimal rounding. *Mathematical Programming Computation*, *6*, 33–54.
- Birge, J., & Louveaux, F. (2011). *Introduction to Stochastic Programming*. Springer Series in Operations Research and Financial Engineering. Springer, New York.
- Bodur, M., & Luedtke, J. R. (2016). Mixed-integer rounding enhanced Benders decomposition for multiclass service-system staffing and scheduling with arrival rate uncertainty. *Management Science*, *63*, 2073–2091.
- Bonami, P., Salvagnin, D., & Tramontani, A. (2020). Implementing automatic Benders decomposition in a modern MIP solver. In D. Bienstock, & G. Zambelli (Eds.), *Integer Programming and Combinatorial Optimization* (pp. 78–90).
- Botton, Q., Fortz, B., Gouveia, L., & Poss, M. (2013). Benders decomposition for the hop-constrained survivable network design problem. *INFORMS Journal on Computing*, *25*, 13–26.
- Charnes, A., Cooper, W. W., & Symonds, G. H. (1958). Cost horizons and certainty equivalents: An approach to stochastic programming of heating oil. *Management Science*, *4*, 235–263.
- Chen, W.-K., Chen, Y.-L., Dai, Y.-H., & Lv, W. (2024). Towards large-scale probabilistic set covering problem: an efficient Benders decomposition approach. In *2024 Informs Optimization Society conference*.
- Cordeau, J.-F., Furini, F., & Ljubić, I. (2019). Benders decomposition for very large scale partial set covering and maximal covering location problems. *European Journal of Operational Research*, *275*, 882–896.
- Daskin, M. S., & Owen, S. H. (1999). Two new location covering problems: The partial p -center problem and the partial set covering problem. *Geographical Analysis*, *31*, 217–235.

- Farahani, R. Z., Asgari, N., Heidari, N., Hosseini, M., & Goh, M. (2012). Covering problems in facility location: A review. *Computers & Industrial Engineering*, *62*, 368–407.
- Fischetti, M., Ljubić, I., & Sinnl, M. (2016). Benders decomposition without separability: A computational study for capacitated facility location problems. *European Journal of Operational Research*, *253*, 557–569.
- Fischetti, M., Ljubić, I., & Sinnl, M. (2017). Redesigning Benders decomposition for large-scale facility location. *Management Science*, *63*, 2146–2162.
- Fischetti, M., & Monaci, M. (2012). Cutting plane versus compact formulations for uncertain (integer) linear programs. *Mathematical Programming Computation*, *4*, 239–273.
- García, S., & Marín, A. (2019). Covering location problems. In G. Laporte, S. Nickel, & F. Saldanha da Gama (Eds.), *Location Science* (pp. 99–119).
- Gendron, B., Scutellà, M. G., Garroppo, R. G., Nencioni, G., & Tavanti, L. (2016). A branch-and-Benders-cut method for nonlinear power design in green wireless local area networks. *European Journal of Operational Research*, *255*, 151–162.
- Güney, E., Leitner, M., Ruthmair, M., & Sinnl, M. (2021). Large-scale influence maximization via maximal covering location. *European Journal of Operational Research*, *289*, 144–164.
- Hu, Z., Sun, W., & Zhu, S. (2022). Chance constrained programs with gaussian mixture models. *IIE Transactions*, *54*, 1117–1130.
- Hwang, H.-S. (2004). A stochastic set-covering location model for both ameliorating and deteriorating items. *Computers & Industrial Engineering*, *46*, 313–319.
- Jiang, N., & Xie, W. (2022). ALSO-X and ALSO-X+: better convex approximations for chance constrained programs. *Operations Research*, *70*, 3581–3600.
- Jiang, N., & Xie, W. (2024). ALSO-X#: better convex approximations for distributionally robust chance constrained programs. *Mathematical Programming*, .
- Klein Haneveld, W. K., Van Der Vlerk, M. H., & Romeijnders, W. (2020). *Stochastic Programming: Modeling Decision Problems Under Uncertainty*. Springer Nature, Switzerland.
- Kleywegt, A. J., Shapiro, A., & Homem-de Mello, T. (2002). The sample average approximation method for stochastic discrete optimization. *SIAM Journal on Optimization*, *12*, 479–502.
- Kuzbakov, Y., & Ljubić, I. (2024). New formulations for two location problems with interconnected facilities. *European Journal of Operational Research*, *314*, 51–65.
- Küçükyavuz, S., & Jiang, R. (2022). Chance-constrained optimization under limited distributional information: A review of reformulations based on sampling and distributional robustness. *EURO Journal on Computational Optimization*, *10*, 100030.
- Lejeune, M. A., & Margot, F. (2016). Solving chance-constrained optimization problems with stochastic quadratic inequalities. *Operations Research*, *64*, 939–957.

- Luedtke, J. (2014). A branch-and-cut decomposition algorithm for solving chance-constrained mathematical programs with finite support. *Mathematical Programming*, *146*, 219–244.
- Luedtke, J., & Ahmed, S. (2008). A sample approximation approach for optimization with probabilistic constraints. *SIAM Journal on Optimization*, *19*, 674–699.
- Lutter, P., Degel, D., Büsing, C., Koster, A. M. C. A., & Werners, B. (2017). Improved handling of uncertainty and robustness in set covering problems. *European Journal of Operational Research*, *263*, 35–49.
- Marchand, H., & Wolsey, L. A. (2001). Aggregation and mixed integer rounding to solve MIPs. *Operations Research*, *49*, 363–371.
- Muffak, A., & Arslan, O. (2023). A Benders decomposition algorithm for the maximum availability service facility location problem. *Computers & Operations Research*, *149*, 106030.
- Nemhauser, G. L., & Wolsey, L. A. (1990). A recursive procedure to generate all cuts for 0-1 mixed integer programs. *Mathematical Programming*, *46*, 379–390.
- Nemirovski, A., & Shapiro, A. (2006). Scenario approximations of chance constraints. In G. Calafiore, & F. Dabbene (Eds.), *Probabilistic and Randomized Methods for Design under Uncertainty* (pp. 3–47).
- Nemirovski, A., & Shapiro, A. (2007). Convex approximations of chance constrained programs. *SIAM Journal on Optimization*, *17*, 969–996.
- Pérez-Galarce, F., Álvarez-Miranda, E., Candia-Véjar, A., & Toth, P. (2014). On exact solutions for the minmax regret spanning tree problem. *Computers & Operations Research*, *47*, 114–122.
- Rahmaniani, R., Ahmed, S., Crainic, T. G., Gendreau, M., & Rei, W. (2020). The Benders dual decomposition method. *Operations Research*, *68*, 878–895.
- Rahmaniani, R., Crainic, T. G., Gendreau, M., & Rei, W. (2017). The Benders decomposition algorithm: A literature review. *European Journal of Operational Research*, *259*, 801–817.
- Ruszczynski, A. (2002). Probabilistic programming with discrete distributions and precedence constrained knapsack polyhedra. *Mathematical Programming*, *93*, 195–215.
- Savelsbergh, M. W. P. (1994). Preprocessing and probing techniques for mixed integer programming problems. *INFORMS Journal on Computing*, *6*, 445–454.
- Saxena, A., Goyal, V., & Lejeune, M. A. (2010). MIP reformulations of the probabilistic set covering problem. *Mathematical Programming*, *121*, 1–31.
- Shen, H., & Jiang, R. (2023). Chance-constrained set covering with Wasserstein ambiguity. *Mathematical Programming*, *198*, 621–674.
- Song, Y., & Luedtke, J. R. (2013). Branch-and-cut approaches for chance-constrained formulations of reliable network design problems. *Mathematical Programming Computation*, *5*, 397–432.
- Toregas, C., Swain, R., ReVelle, C. S., & Bergman, L. (1971). The location of emergency service facilities. *Operations Research*, *19*, 1363–1373.

- Weninger, D., & Wolsey, L. A. (2023). Benders-type branch-and-cut algorithms for capacitated facility location with single-sourcing. *European Journal of Operational Research*, *310*, 84–99.
- Wolsey, L. A. (2021). *Integer Programming*. (2nd ed.). John Wiley and Sons, Inc.
- Wu, H. H., & Kucukyavuz, S. (2019). Probabilistic partial set covering with an oracle for chance constraints. *SIAM Journal on Optimization*, *29*, 690–718.
- Xie, W., & Ahmed, S. (2020). Bicriteria approximation of chance-constrained covering problems. *Operations Research*, *68*, 516–533.